Influence of Synthesis Parameters on the Properties of ZSM-5 & on Their Catalytic Activity for 1-Butene Isomerization

By

Korhan DEMİRKAN

A Dissertation Submitted to the Graduate School in Partial Fulfillment of the Requirements for the Degree of

MASTER OF SCIENCE

Department: Chemical Engineering
Major: Chemical Engineering

İzmir Institute of Technology
İzmir, Turkey

January, 2002

We approve the thesis of **Korhan DEMIRKAN**

Date of Signature

..... **21.01.2002**
Asst. Prof. Dr. Selahattin YILMAZ
Supervisor
Department of Chemical Engineering

..... **21.01.2002**
Prof. Dr. Levent ARTOK
Co-Supervisor
Department of Chemistry

..... **21.01.2002**
Prof. Dr. Muhsin ÇİFTÇİOĞLU
Co-Supervisor
Department of Materials Science and Engineering

..... **21.01.2002**
Prof. Dr. Gönül Gündüz
Department of Chemical Engineering
Ege University

..... **21.01.2002**
Asst. Prof. Dr. Mehtap EMİRDAĞ
Department of Chemistry

..... **21.01.2002**
Asst. Prof. Dr. Fehime ÖZKAN
Department of Chemical Engineering

..... **21.01.2002**
Prof. Dr. Devrim BALKÖSE
Head of Chemical Engineering Department

ACKNOWLEDGEMENTS

I wish to give my thanks to my supervisors, Assistant Prof. Selahattin Yılmaz, Prof. Levent Artok and Prof. Muhsin Çiftçioğlu for their valuable advice, help and support during the course of the research.

Part of this research was carried out at Laboratory of Industrial Chemistry, Faculty of Chemical Engineering, Åbo Akademi University, Turku, Finland. The financial support of Izmir Institute of Technology - Research Fund Accountancy (2000MUH-03) for the research project and the grant of Center of International Mobility (CIMO), Helsinki, Finland are gratefully acknowledged.

My thanks go to Prof. T. Salmi and Prof. D. Murzin for their kind invitation and to the all stuff of Laboratory of Industrial Chemistry for their warm hospitality and friendship. I would especially like to express my appreciation to Docent Narendra Kumar for his endless guidance and help.

The co-operation of N. Akkaya, U. Gunaslan (Quality Control Laboratory, Petkim Petrokimya Refinery Holding A.S.), B. Akyol (Çimentaş A.Ş) and the researchers of Abo Akademi and Izmir Institute of Technology is highly appreciated.

IZMIR, January 2002

Korhan DEMIRKAN

ABSTRACT

The synthesis and preparation of active and selective zeolite catalysts (H-ZSM-5 and H-ZSM-22) for the skeletal isomerization reaction of 1-butene to iso-butene were investigated. H-ZSM-5 zeolite catalysts were synthesized by varying the synthesis time (3, 6, 12, 24, 48 and 72 h), stirring mode (static, rotational), the initial SiO_2/Al_2O_3 ratio (15 , 30, 70) and SiO_2/TPABr (Tetrapropylammonium bromide) ratio (3,3; 5,5; 12,5) of the hydrogel. A synthesis work for H-ZSM-22 type zeolite materials was also carried out both in static and rotational mode. Catalytic activity tests were performed in a constructed fixed bed tubular quartz reactor system at 440 and 375^oC at weight hourly space velocities (WHSV) of 22 and 11 h^{-1}.

The X-Ray Powder Diffraction patterns and Scanning Electron Microscopy images of ZSM-5 zeolites showed that the particle size and phase purity of ZSM-5 increased with increase in synthesis time. The XRD pattern of Na-ZSM-5 zeolite synthesized by the static mode showed a higher degree of crystallization than the rotational synthesis. The sample synthesized with high Al content in the initial hydrogel (SiO_2/Al_2O_3=15) showed less crystallization than the samples synthesized with low Al content. Increasing Si/Al ratio in the synthesis hydrogel resulted in an increase in the surface area (533 m^2/g). TPABr content was found to be an important factor in the crystallization of ZSM-5 zeolites. Lowest TPABr content resulted in an amorphous phase. Increase in the organic cation content enhanced the crystallization, and larger size ZSM-5 crystals with higher phase purity and surface area were achieved. The crystal phase obtained from the hydrogel which was prepared for the synthesis of ZSM-22, were affected significantly by the synthesis mode.

The catalysts prepared were tested for isomerization of 1-butene at 440^oC and 22h^{-1} WHSV. It was found that the hydrogel composition highly influenced the catalytic properties of H-ZSM-5 giving a range of conversion and selectivity for iso-butene. Al rich zeolite (initial SiO_2/Al_2O_3=15) showed very low selectivity (2%). This was attributed to the higher acidity of this zeolite. In contrast the samples having medium and high SiO_2/Al_2O_3 ratios 30 and 70 gave high selectivity (52% and 56% respectively) and yield (26% and 28% respectively) under the same reaction conditions.

The sample with initial SiO_2/Al_2O_3=30, SiO_2/TPABr= 3.3 gave the highest yield to iso-butene (28%) under the same reaction conditions (440^oC , 22h^{-1}). Reaction at a lower temperature (375^oC) increased iso-butene yield to 32% by suppressing the by-product formation. Decreasing the WHSV (11 h^{-1}) increased conversion from 40% to 48% and giving yield of 32% iso-butene. The test for long time on stream (24 h) to asses catalytic deactivation, showed slight increase in the yield of iso-butene (%33).

ÖZ

Bu çalışmada 1-butilen iskelet izomerizasyonu reaksiyonu için aktif ve seçici ZSM-5 ve ZSM-22 katalizörlerinin sentezlenmesi ve hazırlanması araştırılmıştır. Farklı H-ZSM-5 zeolitleri, sentez süresi (3 , 6, 12, 24, 48 ve 72 saat), sentez şekli (statik ve karıştırmalı), sentez jelindeki SiO_2/Al_2O_3 (15, 30, 70) ve SiO_2/TPABr (tetrapropilamonyum bromür) oranları (3,3; 5,5; 12,5) değiştirilerek sentezlenmiştir. H-ZSM-22 zeolit malzemesi için de statik ve karıştırmalı ortamda sentez çalışmaları yapılmıştır. Katalizörlerin aktiflikleri kurulan bir sabit yataklı reaktör düzeneğinde 440 ve 375^oC'de test edilmiştir.

X-Ray Kırınm (XRD) desenleri ve taramalı elekron mikroskobu (SEM) görüntüleri ZSM-5 zeolitlerinde, parçacık boyutunun ve faz saflığının sentez süresi uzadikça arttığını göstermiştir. Statik ortamda sentezlenen ZSM-5 zeolitinin XRD deseni, karıştırmalı ortamda sentezlenen zeolit örneğinden daha yüksek derece kristalleşme göstermiştir. Yüksek Al miktarı (SiO_2/Al_2O_3=15) ile sentezlenen örnek daha düşük kristal oluşumu göstermiştir. Jeldeki Si/Al oranı arttıkça sentezlenen örneklerin yüzey alanları artış göstermiştir (533 m^2/g). TPABr miktarının ZSM-5'in kristalleşmesi için önemli olduğu belirlenmiştir. TPABr miktarının en düşük olan örneğin XRD deseni amorf fazın varlığını göstermiştir. Fakat organik katyon miktarı arttıkça kristalleşme artmış, daha büyük, daha saf ve daha fazla yüzey alanına sahip ZSM-5 kristalleri elde edilmiştir.

Hazırlanan katalizörler 1-büten'in izomerleşme reaksiyonu için 440^oC'de test edilmiştir. Sentez jeli kompozisyonun H-ZSM-5 katalizörlerinin katalitik verimliliklerini yüksek derecede etkilediği bulunmuştur. Al miktarınca zengin olan (SiO_2/Al_2O_3=15) katalizör örneği çok düşük izobutilen seçimliliği sağlamıştır (2%). Bunun aksine sentez jelindeki SiO_2/Al_2O_3 oranı 30 ve 70 olan katalizörler aynı reaksiyon koşulları altında yüksek dönüşüm ve izobutilen seçimliliği sağlamıştır. Sentez jelindeki SiO_2/Al_2O_3=15 ve SiO_2/TPABr=3,3 olan katalizör aynı reaksiyon koşulları altında (440^oC, 22h^{-1}) en yüksek izobutilen verimi (%28) sağlamıştır. Daha düşük sıcaklıkta (375^oC) yapılan test yan ürünlerin oluşumunu azaltmış ve izobutilen verimini %32'ye arttırmıştır. Katalizör miktarının iki katına arttırılması, elde edilen verimi (%32)

değiştirmemiştir. Katalizörün aktifliğindeki değişimi belirlemek için 24 saat boyunca yapılan testte izobutilen verimi (%33) çok az artış göstermiştir.

TABLE OF CONTENTS

LIST OF TABLES

LIST OF FIGURES

CHAPTER I

INTRODUCTION

Skeletal isomerization of 1-Butene is an important process as an alternative route to thermal cracking for the production of iso-butene. Iso-Butene is a very demanded petrochemical for the production of methyl tert-butyl ether (MTBE), which is used as an octane booster in lead free gasoline.

The main by-products of the conversion of 1-butene are 8 carbon oligomers formed by the dimerization of butenes. Zeolite catalysts can suppress the formation of 8 carbon oligomers within a suitable pore structure. But the pore structure is not enough for achieving high selectivity and yield to iso-butene. The number and the strength of the acid sites present in the zeolite structure is another major condition for achieving high selectivity and yield. So the acidity of the zeolite catalysts has to be sensitively adjusted since catalysts having low acidity leads to very low conversions of 1-Butene and on contrary, high acidity may exhibit higher conversion but promotes the formation of several undesired by-products (Houzvicka et al, 1998).

In literature, the potential catalytic applications of synthetic zeolites and aluminophosphates have been demonstrated for 1-Butene skeletal isomerization reaction, but fast deactivation is unavoidable for many of the active and selective catalysts. Therefore a desire for high coke resistance as well as high activity and selectivity still exits.

Mobil Corp.'s ZSM-5 (Zeolite Scony Mobil-5) catalyst or officially named MFI (Mobil-Five) catalyst is the most versatile of zeolite catalysts (Meisel, 1984) because of its high thermal stability and coke resistance. Therefore, in this thesis study, the acidity of the ZSM-5 catalyst is tried to be adjusted by varying the synthesis parameters, and the optimum synthesis conditions are tried to be identified for ZSM-5 catalysts that will be used in 1-Butene skeletal isomerization reaction.

CHAPTER II

SKELETAL ISOMERIZATION OF N-BUTENE OVER ZEOLITE CATALYSTS

2.1. SKELETAL ISOMERIZATION OF LINEAR-BUTENES

Iso-butene is a highly demanded petrochemical, which is used as the raw material for the manufacture of methyl tert-butyl ether (MTBE). Essentially the success of MTBE is founded on its outstanding antiknock properties with a high octane number (octane number: 118) (Moulijn et al. 1993.) and it is the most largely used quality improving additive for unleaded gasoline. MTBE can easily be produced by the reaction of iso-butene and methanol over an acidic zeolite catalyst (Collignon et al. 1997; Nikolpoulos et al. 1996) but this production is limited with the supplies of iso-butene.

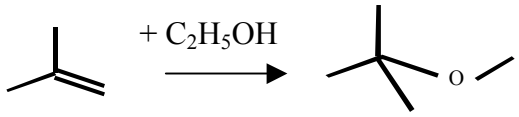

Iso-butene MTBE

Isobutene is also an important feed stock in the production of isoprene and methacrylic acid, which are used as additives in the polymer industry (Simon et al. 1994).

There are around 28% 1-Butene and 12% 2-Butene in spent C_4 refinate and the conversion of 1-butene and 2-butene to iso-butene is a convenient alternative way of producing more iso-butene to fulfill the demand (Yang et al. 1999). This conversion has been of considerable interest recently.

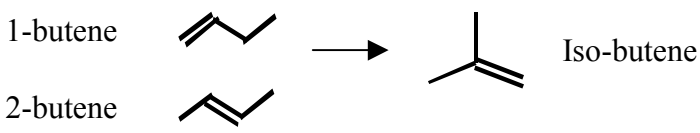

Skeletal isomerization of linear butenes to isobutene is a reversible reaction and it is not thermodynamically so favored. Although this transformation is an exothermic reaction, kinetics and the formation of by products limit the possibility of using low temperatures. The optimum operating temperature strongly depends on the catalyst, and as the acidity is reduced, there will be an increase for the optimum operation temperature. It is known that the formation of the by products are strongly exothermic, so decreasing the temperature, increases the by-product formation and decreases the yield of isobutene. At temperatures above 460^{o}C the thermodynamic equilibrium becomes less favorable for I-C_4H_8 so high temperatures are also not applicable. The optimum reaction temperature is always in the range between 300 and 480^{o}C (Simon et al. 1994).

Conversion of 1-butene to iso-butene is achieved in two different reaction mechanisms (Houzvicka et al. 1996; Cejka et al. 1999; Seo et al. 1998):

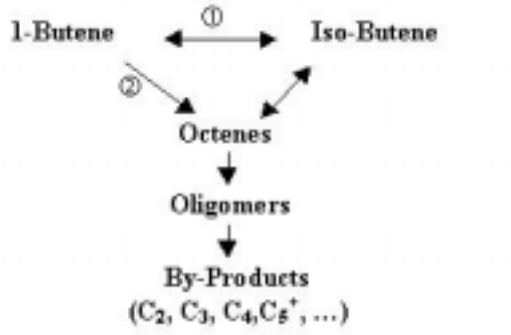

① Monomolecular Mechanism
② Bimolecular Mechanism

First is the monomolecular mechanism which is the skeletal isomerization of 1-butene to iso-butene. Second is the bimolecular mechanism that n-butene or iso-butene or both oligomerize forming C_8 products that are prompt to crack leading mainly to propylene and pentenes and minor amount of iso-butene (Asensi et al. 1998). The consecutive and parallel reactions occuring during the bimolecular mechanism have a detrimental effect on iso-butene selectivity.

The acid strength required for acid catalyzed conversions of hydrocarbons can be ranked as Cracking Oligomerization> Skeletal Isomerization>> Double Bond

Isomerization. Therefore, an ideal skeletal isomerization catalyst should have an acidity that is strong enough for skeletal isomerization but not strong for oligomerization and cracking (Canizares et al, 2000).

It is investigated that the character of the acid sites, namely Brönsted and Lewis, are considered to affect the reaction pathway. Simultaneous presence of Brönsted and Lewis sites in zeolite lead to enhanced acidic activity of zeolites in hydrocarbon transformations (ethylene oligomerization and hexane cracking). For 1-butene isomerization reaction, lewis sites, if present with Brönsted sites in the zeolite, enhance dimerization and oligomerization of butenes. The formation of isobutene by skeletal isomerization of n-butenes was found to be proportional to the concentration of Brönsted sites present in 10 member ring main channels of zeolites accessible to iso-butene molecules (Cejka et al, 1999).

The reaction path of the monomolecular mechanism over Brönsted sites is suggested to be as given in Figure 2.1. (Bygnningsbacka et al. 1997):

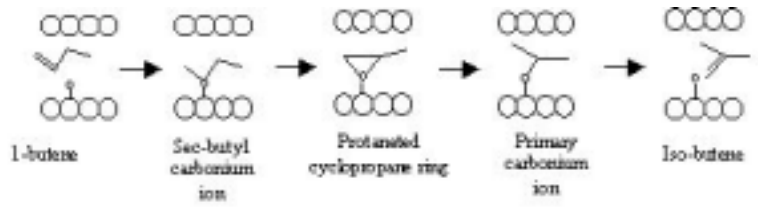

Figure 2.1. Transformation of 1-Butene to iso-butene through suggested monomolecular mechanism over zeolite catalyst.

Unique pore structure of zeolites is very suitable for this conversion by suppressing the formation of 8 carbon oligomers in the pore structure of zeolites. The previous studies showed that open surface oxidic materials such as alumina and WO_3 deactivate very fast and can not suppress the formation of the by products, therefore the zeolites have been very superior to amorphous structures for the suppression of the side reactions and achieving higher reaction yields.

The pore structure of the zeolite is a very important parameter for high iso-butene selectivity. A restricted pore size limits the dimerization and polymerization reactions. If the molecular size of the reactant 1-butene (3.0 x 4.7 Å) and the product isobutene (3.3 x 4.1 Å) are taken into consideration, the zeolites to be used in the skeletal isomerization of 1-butene should have at least 4.3-6.0 Å channels which corresponds to 10-oxygen-membered ring structure.

The channels of 8-oxygen-membered ring zeolites (3.5-4.5 Å) are found to be too small to allow branched molecules to diffuse with any considerable rate, which results in a rapid deactivation of the catalyst. On the other hand, the 12-membered ring zeolites (6.0-8.0 Å) did not suppress the formation of carbonaceous deposits and their pores were quickly blocked. Since 10-membered ring zeolites (4.5-6.0 Å) allow iso-butene diffusion and also prevented extensive oligomer formation inside narrower pores as illustrated in Figure 2.2. (Houzvicka et al, 1997), bimolecular reactions are favored less over the 10-membered zeolites.

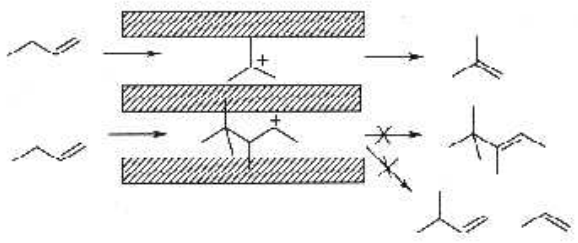

Figure 2.2. Restricted transition state selectivity prevents bimolecular reactions producing octenes, propene, and pentenes.

Furthermore there appear to be large differences in product selectivity between 10 MR zeolites depending on the particular topology of the zeolite structures. The pore structure of various 10 oxygen membered zeolites are illustrated in Figure 2.3.

Figure 2.3. Illustrations of three-dimensional pore structures of ZSM-5, ZSM-22 and ZSM-11.

For instance, unidirectional 10MR zeolites such as theta-1, ZSM-22, ZSM-23 are generally found to be more selective than ZSM-5 and ZSM-11, the later having a bidirectional system of intersecting 10 MR channels.

The lower selectivity to isobutene over ZSM-5 compared to ZSM-22 was owing to the intersections of ZSM-5's channels. The cavities of ZSM-5 zeolite could not prevent dimerization reactions, and offer enough space for oligomerization. ZSM-5 results in higher selectivity especially to propene and pentenes. The product distribution over ZSM-11 was almost identical to ZSM-5, since both of them have cavities of similar size.

2.2. MOTIVATION OF THE RESEARCH

The catalysts known for this reaction at the moment are not yet optimal. As a result of thermodynamical limit at high reaction temperatures, the iso-butene yield on the best contemporary catalysis is only about 40%. This low yield simulates a further research for novel catalysis.

Another main problem is the rapid deactivation of the catalyst because of coke formation (polymerization of butenes starting via dimers), which lead to blockage of pores. From the industrial point of view, the cost of this deactivation is very high and great efforts have been made to find methods, for limiting the formation of coke and its effect on the zeolite activity (Guisnet et al. 1992).

ZSM-5 has an incredible high thermal stability towards amorphization and dealumination. Since the three-dimensional channel structure always lets available paths for adsorption and desorption for the species, the resistance of this catalyst against coking is much higher than that of one-dimensional molecular sieves (Figure 2.4.).

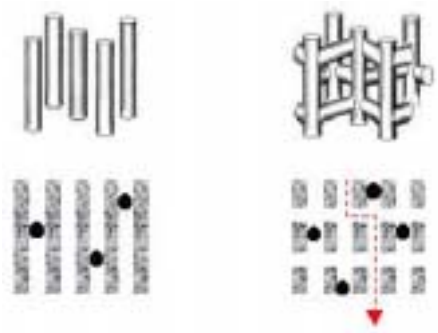

Figure 2.4. Coke formation (a) in noninterconnecting channel systems and (b) in three-dimensional channel system (Hölderich et al. 1991).

Therefore, modifying the acid strength of ZSM-5 as a potential way to increase the selectivity can be a very appreciated result for industry (Houzvicka, et al, 1997).

CHAPTER III

BACKGROUND: ZEOLITE CATALYSTS

3.1. INDUSTRIAL IMPORTANCE OF ZEOLITE CATALYSTS

Zeolites occur in nature and have been known for almost 250 years as aluminosilicate minerals. Most common examples are clinoptilolite, faujasite, mordenite, ferrierite and chabazite. Today these and other zeolite structures are of great interest in many fields. Catalysis is the most important application of zeolites in terms of financial market size (not in terms of tons of production per year) (Weitkamp et al, 1999).

Zeolite catalysts exhibit unusually high activity for various acid catalyzed reactions. Several important properties of zeolite catalysts that are not found in traditional amorphous catalysts can be listed as follows:

1. Zeolites have porous crystal structures made up of channels and cages that allow a large surface area thus a large number of catalytic sites. Zeolites can accommodate as many as 100 times more molecules than the equivalent amount of amorphous catalyst.
2. Zeolites are strong acid catalysts due to a large proportion of Bronsted acid sites scattered throughout their porous structure.
3. Since they are solid, they are easily removable from products and therefore they are environmental friendly.
4. Furthermore their molecular sieve action can be exploited to control which molecules have access to or which molecules can depart from the active sites which is defined as shape-selectivity.

But unfortunately from the catalytic point of view, their naturally occurring forms are of limited value, because (Weitkamp, 2000).

1. They almost always contain undesired impurity phases,

2. Their chemical composition varies from one deposit to another and even from one stratum to another in the same deposit and
3. Nature did not optimize their properties for catalytic applications.

Studies on synthesizing of new zeolite structures and their catalytic applications showed an incredible growth so far from the first discovery of synthetic zeolites (Bhatia, 2000). Today about eighty structurally different synthetic zeolites are known, and some of them have great practical significance in many catalytic applications. Table 3.1. lists some maturing, developing and emerging applications of zeolite catalysts.

Table 3.1. Maturing, developing and emerging applications of zeolite catalysts.

Maturing	**Developing**	**Emerging**
Fluid Catalytic Cracking (FCC)	Hydrocracking	Reforming
Methanol to Gasoline	FCC Additives	Iso-Dewaxing
Paraffin Isomerization	Xylene Isomerization	Auto Exhaust
Ethylbenzene Alkylation	Oxidation H_2O_2	De-NO_x
Catalytical Dewaxing	Hydrogenation	
	1-Butene Isomerization	

In the Petroleum Refining area, the catalytic cracking (Zeolite Y, ZSM-5) is by far the largest application in petroleum refining area that is followed by hydrocracking catalysts (Y, Mordenite). Other applications are in hydro-isomerization and dewaxing, using mostly mordenite and ZSM-5. The well known Methanol-To-Gasoline process for synfuel production applies ZSM-5. Also important petrochemical processes such as ethylbenzene by alkylation of benzene, xylene isozmerization, toluene disproportionation run over ZSM-5 contaiing catalysts (Moscou, 1991; Sherman, 1999).

The use of zeolite catalysts in the production of organic fine chemicals is appearing as a major new direction, and there have been many studies devoted recently (Davis, 1998).

3.2. ZEOLITE CHEMISTRY

3.2.1. Chemical Structure

Zeolites comprise a three-dimensional crystal network of Si and Al atoms that are present in the form of SiO_4 and $[AlO_4]^{-1}$ tetrahedra. Tetrahedrals join together in through shared oxygen atoms with various regular arrangements, to form hundreds of different three-dimensional crystal frameworks (Figure 3.1.). The framework structure encloses cavities containing pores of molecular dimensions into which some molecules can easily penetrate.

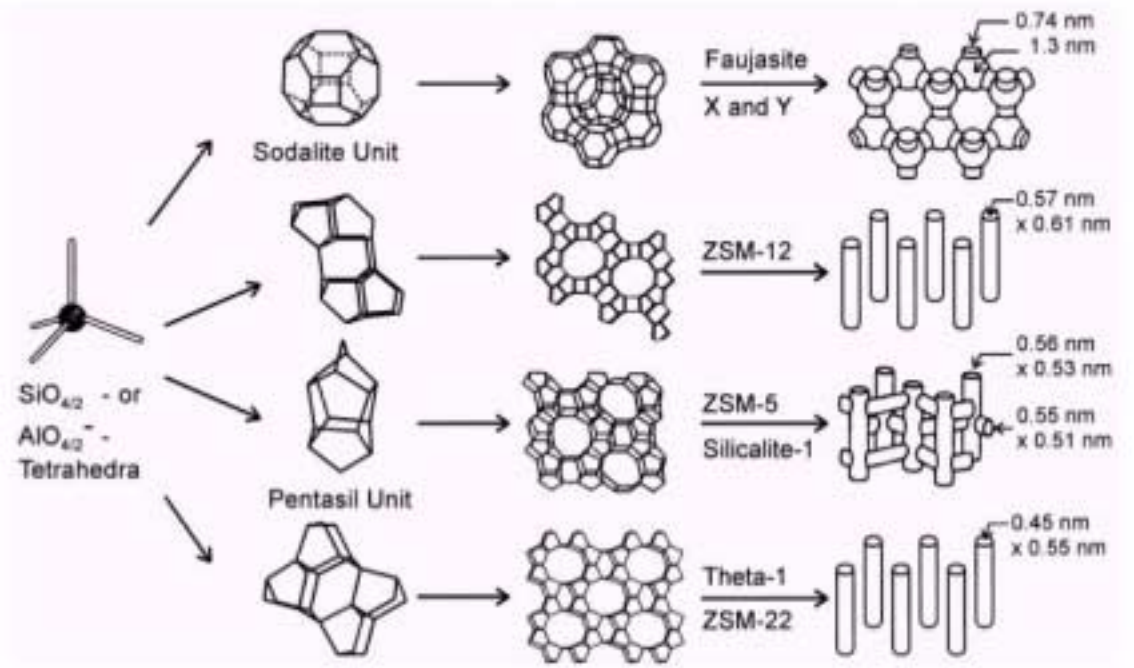

Figure 3.1. SiO_4 and AlO_4 building block of zeolites (Weitkamp, 2000).

3.2.2. Surface Chemistry

The characteristic that separates zeolites from all-silica minerals, is the substitution of metals other than silicon into the crystalline framework, which is aluminium in this case. The replacement of SiO_4 tetrahedra by the $[AlO_4]^{-1}$ tetrahedra in the zeolite framework causes excess negative charges and cationss are needed to neutralize them. Compensation of the negative charge by associated cations such as H^+, Na^+, K^+, Ca^{2+},

NH_4^+ generates the acid sites. The catalytic activity of the zeolites is attributed to the presence of these acidic sites and the proton affinity at the charged framework. The catalytic activity of acid sites may be Bronsted or Lewis in character (Hindle, 1997).

If the charge compensating cation associated with the thetrahedral aluminum is hydrogen, the zeolite surface obtains the capacity to act as a proton donor and therefore can serve as a Bronsted acid:

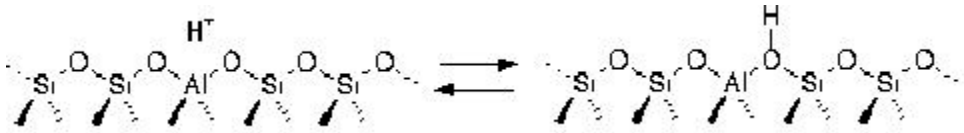

If the zeolite is heated to a temperature higher than 550^oC formation of Lewis acid site and zeolitic water occur. According to model of Ward (Ward, 1996) two Bronsted acid sites are required to form a single Lewis (electron acceptor) acid site:

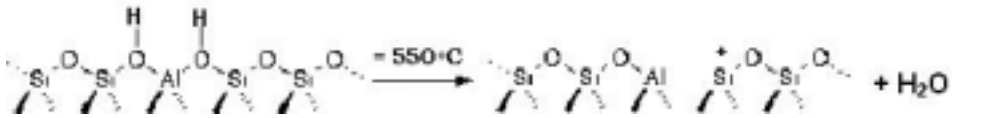

Both type of acid sites are responsible for the carbonium ion based chemistry of zeolite catalysts. If transition metals are introduced into the zeolite by conventional ion exchange techniques, a third type of active site can be generated.

3.2.3. Pore Structure and Molecular Sieving

There are two types of pore structures of zeolites, one provides an internal pore system comprised of interconnected cage-like voids, e.g. Zeolite A and Zeolite Y, the other provides a three dimensional system of uniform channels, e.g. ZSM-5 has set of straight, parallel pores intersected by a set of perpendicular zigzag pores, or in some instances as ZSM-22, composed of only straight parallel pores, it can be one-dimensional channel systems (Figure 3.1.).

The crystalline voids make up from 20 to 50% of the crystal volume of most zeolites (Zeolites A, X and Y have void volume near 50%) (Breck, 1974).

The diameters of the windows or pore leading into the voids range from 3 to 10 Å depending on the arrangement of the tetrahedral units. The number of oxygen atoms exist in the ring determines the size of aperture. The apertures can have 8, 10 or 12 oxygen atoms and zeolites are classified according to this number of oxygen atoms as 8, 10 or 12 oxygen membered ring zeolites as shown in Figure 3.2.

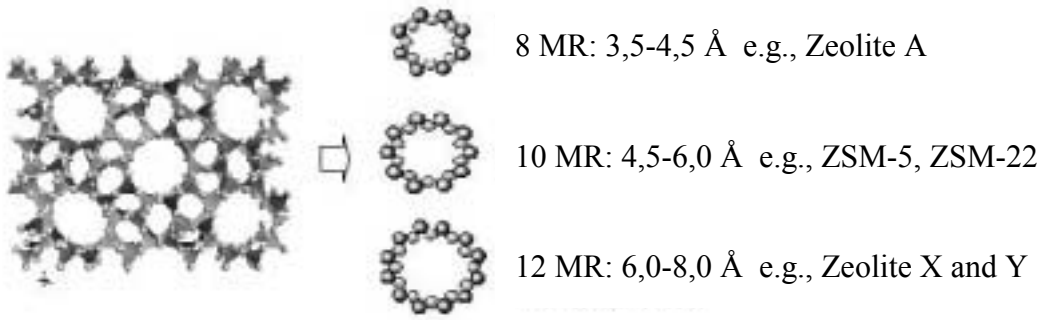

Figure 3.2 Schematic presentation of the terahedrals forming 10 oxygen membered ring aperture of ZSM-5 structure (left). 8, 10 and 12 Oxygen Membered Rings (MR) are depicted schematically (right).

The size of the aperture is also dependent on the sizes of the nearby cations, which may partially block it. Kinetic diameters of some simple molecules are illustrated on Figure 3.3.

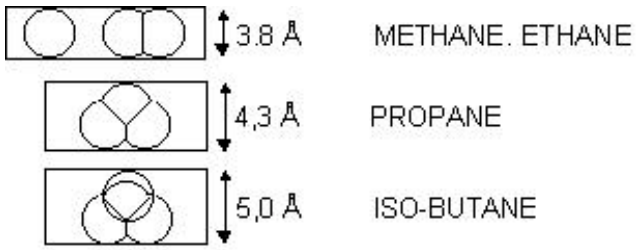

Figure 3.3. Illustration of the kinetic diameters of some simple molecules (Clifton, 1987)

Today computer modellings are extremely useful for illustrating whether a molecule is able to pass through a pore opening or channel (Millini, 1998). Figure 3.4. is a simple illustration of molecular sieving ability of an 8 oxygen membered ring zeolite.

Figure 3.4. Illustrations of molecular sieve effect. Straight chain molecule of normal octane (left) passes through an eight-ring zeolite; branched molecule of iso-octane (right) cannot (Falnigen. 1991).

Shape selectivity is the ability of a zeolite to restrict or prevent the passage of molecules based on size. There are three different types of shape selectivity observed associated with zeolites as shown in Figure 3.5.:

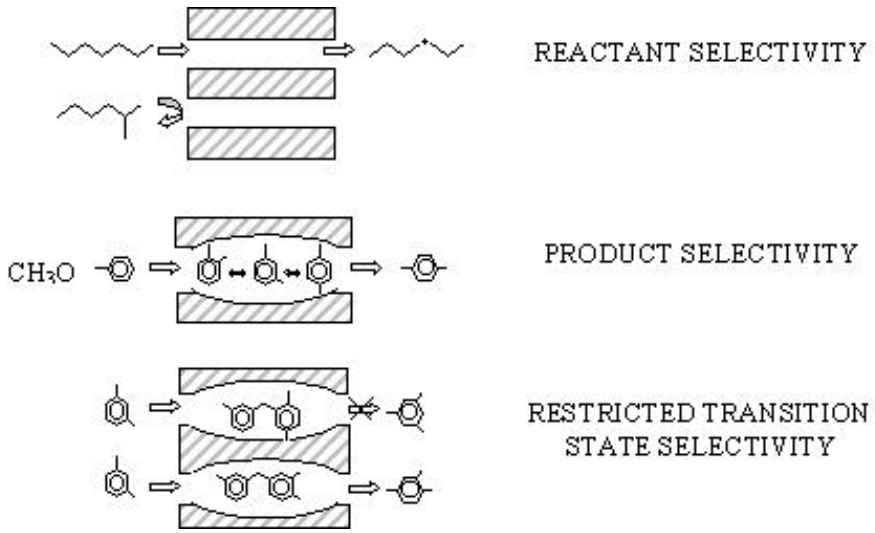

Figure 3.5. Illustration of reactant, product and restricted transition state selectivity of zeolites.

1. Reactant selectivity occurs when some of the molecules in a mixture are too large to diffuse through the catalyst pores.
2. Product selectivity occurs when some of the products formed within the pores are too bulky to diffuse out as observed products. The bulky molecules are either converted to less bulky molecules or to coke that eventually deactivate the catalyst.
3. Restricted transition state selectivity occurs when certain reactions are prevented because the corresponding transition state would require more space than available

in the cavities or pores. Reactions requiring smaller transition states proceed unhindered.

3.3. ZEOLITE SYNTHESIS

Zeolites are synthesized hydrothermally in highly alkaline (pH=11-14) gel solutions containing aluminate and silicate anions. Mostly the synthesis is carried out in batch systems. General conditions for synthesis can be summarized as (Breck, 1974):

1. Reactive starting materials such as freshly co-precipitated gels, or amorphous solids.
2. Relatively high pH introduced in the form of an alkali metal hydroxide or other strong base.
3. Low temperature hydrothermal conditions with concurrent low autogenous pressure at saturated water vapor pressure.
4. A high degree of supersaturation of the component of the gel leading to the nucleation of a large number of crystals.

The first step involves the dissolution of the aluminum and silicon to form aluminate and silicate anions. These are then brought together to form a gel, through the result of condensation/polymerization-type reaction. The gel is maintained for a period of time at a constant pressure and temperature in the presence of large excess water. The simultaneous reactions that occur during this period can be summarized as: Precipitation of a gel phase, dissolution of the gel, nucleation of zeolite, continued crystallization and crystal growth of the zeolites.

The nature of the starting material, temperature, pH, aluminate, hydroxl and silicate ion concentrations, gel aging and other species present in solution i.e. alkali cations are each important in determining the resulting zeolite product. Furthermore, there are other physical variables such as order of mixing, rates of addition of aluminate to silicalite solution, and rate of agitation, which also affect the chemistry of the species.

3.3.1. Preparation of the Gel

The first condition for the synthesis is the formation of an aluminosilicate gel composed of silica source, alumina source, cation source and water. The function of the silica and alumina is to form the structure and the cation is needed to compensate the negative charge of alumina, therefore any silica, alumina and cation source can be used: For example fumed silica, colloidal silica, sodium silicate, sodium waterglass, silica gel are used as Si source and alumina powder, aluminum hydroxide, sodium aluminate, aluminum sulfate, aluminum nitrate are commonly used as Al source.

Commonly shortly after mixing the Si, Al and cation sources, it become viscous due to the formation of alumina-silicate gel suspension in the basic medium (Thompson, 1998). Generally, additionally a specific organic cation is added after the gel formation. These organic cations used to template particular framework structure with their ability of altering the course of a crystallization process and are often the dominant factors determining which zeolite structure is obtained. Addition of such organics to the reaction mixture also enhances the crystallization rate, and alters the crystal size (Rollmann, 1984).

For achieving particular crystalline structures always a range of compositions are presented. The primary composition source in zeolite synthesis is the patent literature. Framework compositions can often be varied by simply changing the SiO_2/Al_2O_3 ratio of the reaction mixture. For example, ZSM-5 can be easily prepared with variable SiO_2/Al_2O_3 ratios from 5 to 100 (Rollmann, 1984). Table 3.2. represents the range of variable ratios resulting with highly ZSM-5 phase.

Table 3.2. The broad, preferred and particularly preferred ranges of composition of reaction mixtures which yield the ZSM-5 phase (Argauer et al. 1972).

Ratio	Broad	Preferred	Particularly Preferred
OH^-/SiO_2	0,07 – 10,0	0,1 – 0,8	0,2 – 0,75
$TPA^+/(TPA^+ + Na^+)$	0,2 – 0,95	0,3 – 0,9	0,4 – 0,9
H_2O/OH^-	10 – 300	10 – 300	10 – 300
SiO_2/Al_2O_3	5 – 100	10 – 60	10 - 40

3.3.2. Nucleation and Crystallization

The gels are crystallised in a closed hydrothermal system at temperatures varying generally from room temperature to about 200^{o}C. The pressure is generally the autogenous pressure and approximately equivalent to the saturated vapor pressure of water at the temperature designated. The time required for crystallization varies from a few hours to several days.

Amorphous gel has a thermodynamic tendency to dissolve, while the thermodynamic driving force is toward formation of the crystalline zeolite phase. As the synthesis proceeds at elevated temperature, zeolite crystals are formed by a nucleation step, and the zeolite nuclei then grow larger by assimilation of alumina-silicate material from the solution phase. Therefore, zeolite crystallization is a nucleation-controlled process and the growth of crystalline aluminosilicates first requires the formation of a nucleus. Assimilation of mass from the solution and its reorientation into ordered zeolite may be in form of further nucleation, or grow instead of nucleating more new crystals, which is difficult to predict (Rollmann, 1984) .

Zeolite crystal growth stops when sufficient material has been deposited to reduce the solution concentration to the zeolite equilibrium level (Thompson, 1998).

Most of the synthesis comprises, organic templated synthesis, the use of an organic template molecule as a structure-directing agent. Template-free synthesis is also achieved to prevent the use of these expensive and corrosive agents but this frequently requires higher crystallization time and/or seeding procedures. It is also known that, the wide compositional range for templated synthesis is not applicable for the non-templated synthesis. Template free synthesis of ZSM-5 is limited with a silica to alumina ratio. (Ohayon et al, 2001).

In a templated synthesis, the aluminosilicate gel dissolves and the silica and alumina re-orients and crystallize around the organic template. The structure of the organic species has a dominant factor determining the resultant crystal phase. Whereas tetra-propyl species (e.g., tetra-propyl ammonium hydroxide, tetra-propyl ammonium bromide) are commonly used for the synthesis of ZSM-5, di-amine species (e.g., di-

amino hexane, di-amino heptane) are found to be most effective template agents for the synthesis of ZSM-22 type crystals (Figure 3.6.).

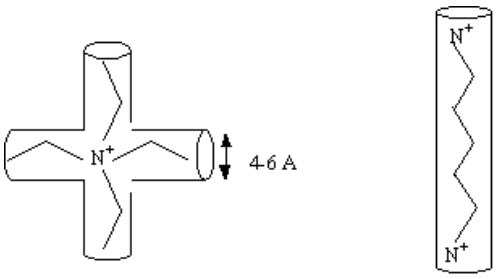

Figure 3.6. Illustration of tetra-propyl and di-amine species (Vartuli, 1998).

3.3.3. Calcination

After filtering and washing, the zeolite is obtained with the terapropyl ammonium ion still present in the zeolite framework (1 TPA per pore intersection). The organic template in the pores of the crystallized samples has to be removed for achieving a high surface area. This can be done by heating it around 500^{o}C. Generally all the organic templates decomposes at temperatures between 360-550 ^{o}C (Howden, 1982). After the calcination, what obtained is the zeolite in which Na^{+} is still present. Different calcination techniques and their effects on the zeolite acidities can be found in literature (Byggningsbacka et al, 1997).

3.4. MODIFICATION OF ZEOLITES FOR CATALYTIC APPLICATIONS

Catalytic properties of zeolites depend on several factors including the presence of active sites, e.g. acidic, basic or cationic sites, the spatial arrangement and size of channels and cavities and the presence of extra compounds within the channels or on the outer part of the crystallites. Changing one or several of these factors may affect the catalytic properties (Vedrine, 1992).

Zeolites as normally synthesized usually have Na^{+} ions balancing the framework charges, but these can be readily exchanged for protons by direct reaction with an acid, giving surface (-OH) hydroxyl groups-the Bronsted sites. Alternatively, if the zeolite is not stable in acid solution, it is common to form the ammonium, NH_4^{+}, salt, and then

heat it so that ammonia is driven off, leaving a proton. Further heating removes water from the Bronsted site, exposing a tricoordinated Al ion, which has electron-pair acceptor properties; this is identified as a Lewis acid site. The surfaces of zeolites can thus display either Bronsted or Lewis acid sites, or both depending on how the zeolite is prepared. Bronsted sites are converted into Lewis sites as the temperature is increased above 600 ^{o}C, and water is driven off.

A widely recognized modification is to replace the Na^{+} ions with other metal ions such as Ni^{2+}, Pd^{2+} or Pt^{2+} and then reduce them in situ so that metal atoms are deposited within the framework. The resultant material displays the properties associated with a supported metal catalyst and extremely high dispersions of the metal can be achieved. Ion exchanged cation can induce new catalytic features either by their different size or by their specific chemical features.

A similar modification corresponds to the addition of a given compound at sites located inside the channels or cavities of the crystallites. This results in a change in active site density, in active site strength distribution in the accessibility of reactants to these sites and in reactant or product molecules diffusivities throughout the channels and cavities. (Imelik et al, 1994)

Another modifications include isomorphous substitution of aluminium or silicon by another trivalent (B, Cr, Ga, Fe) or tetravalent V, Ti elements. This results mainly in changes in acidic and thus in catalytic features. Such a modification can be performed either by direct synthesis by adding the appropriate salt in the medium or by post synthesis modification, such as the use of halides such as $SiCl_4$, BCl_3, PCl_5, $TiCl_4$, $SnCl_4$, VCl_5, NH_4F or $LaCl_3$.

The last but not the least is the dealumination of the zeolite framework. This is carried out either by hydrothermal treatment followed by hydrochloric acid leaching. Depending on the dealumination procedure local Al vacancies may be formed or local atoms rearrangement may occur resulting in the formation of holes and therefore of a mesoporosity.

3.5. CHARACTERIZATION OF ZEOLITES FOR CATALYTIC APPLICATIONS

Before a zeolite catalyst can be used for any certain application it is necessary to characterize the zeolite, to see if it has the desired properties for that application. If not, another synthesis method should be used or the zeolite must be modified, to meet the specifications. Zeolite synthesis, modification, characterization and application thus are strongly related to each other as schematically indicated in Figure 3.7. Characterization is the feedback control for further progression in zeolite synthesis.

There are many ways to obtain information on the physico-chemical properties of zeolite based material catalysts (Imelik et al, 1994). The common techniques used in catalysis are summarized below.

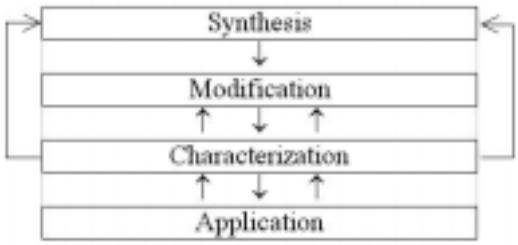

Figure 3.7. Position of Zeolite Characterization (Hooff et al, 1991).

3.5.1. Phase Analysis and Zeolite Structure

It is very important that the zeolite has the correct structure and has no structural defects. Zeolite identification is made largely on the basis of X-ray diffraction technique (XRD). This is obviously the best technique to characterize which type of material is involved in a given sample (Vedrine, 1992).

X-Ray diffraction is the elastic scattering of X-Ray photons by atoms in a periodic lattice. By varying the angle θ, the Bragg's Law ($N\lambda=2d\sin\theta$) conditions are satisfied by different d-spacing in crystalline material. Plotting the angular position and intensities of the resultant diffracted peaks of radiation, produces a pattern which is

characteristic of the sample and allows identifying the material when its structure and XRD pattern are already known. Powder patterns are the common measure of purity in a crystallization product by comparing with an reference spectra. Particle size can also be estimated since large crystallites give rise to sharp peaks, while the peak width increases as crystallite size reduces.

3.5.2. Sorptive Properties and Pore structure

Sorptive properties are an important measure of product integrity among well-characterized zeolites. Surface area and pore size distributions are of primary importance when characterizing the microstructure of porous solids. Characterization method is based on the low temperature gas adsorption of N_2 or CO_2. From complete adsorption and desorption isotherms, pore size/pore volume distribution and specific surface area can be determined.

3.5.3. Surface Imaging

Electron microscopy is an essential ingredient in product characterization. Particle size and morphology are both important, controllable aspects of a synthesis work. Scanning Electron Microscopy (SEM) provides a direct image of the topographical nature of the surface from all the emitted secondary electrons. Transmission electron Microscopy (TEM) which is also a very essential technique, which uses transmitted and diffracted electrons. Whereas SEM sees contrast due to the topology of a surface, TEM projects all information in a two-dimensional image, which however is of sub nanometer resolution (Niemantsverdriet, 1993).

3.5.4. Surface Acidity

For a complete zeolite acidity characterization, it is necessary to determine number and strength of both types of acid sites, Bronsted and Lewis. Several methods exists for this purpose, from which the most important are IR spectroscopy and Temperature Programmed Adsorption and Desorption of bases.

In situ FT-IR analysis of absorbed bases is one of the most common characterization application giving comparative idea about the surface acidity, Bronsted and Lewis sites present in the sample. Frequently the reaction with pyridine is used for this purpose. The reaction on the Bronsted acid site results in the formation of a pyridinium ion while the pyridine molecule is cooridnatively bound on the Lewis acid site of the zeolite (Hooff et al, 1991). Both pyridinium ion and the coordinatively bound pyridine have characteristic IR absorption bands. In this way it is possible to indicate the presence of both Bronsted and Lewis acid sites in zeolite samples whilst the intensity of the band gives information on the number of these sites. It is however, impossible to obtain information on the acid strength.

Temperature Programmed Techniques are applied to gain idea about the strength of the acid sites. This simple technique is based on adsorption of one or more molecular species onto the sample surface at low temperature and heating of the sample in a controlled manner (preferably so as to give a linear temperature ramp) whilst monitoring the evolution of species from the surface back into the gas phase. The area under a peak is proportional to the amount originally adsorbed, i.e. proportional to the surface coverage and the position of the peak (the peak temperature). The peak temperature is related to the enthalpy of adsorption i.e. to the strength of binding to the surface.

3.5.5. Elemental Analysis

The methods for the determination of the chemical composition can be by complete dissolution of the zeolite and subsequent analysis (e.g., Inductive Coupled Plasma, X-Ray Flourescency, Atomic Adsorption Spectroscopy) or direct analysis of the solid material by physical methods (e.g., Nuclear Magnetic Resonance, X-Ray Photoelectron Spectroscopy)

The framework Al content may be quite different from the overall Al content of a zeolite. ^{29}Si NMR is sensitive to the nature of substituents present in the second coordination shell of silicon and makes possible the determination of the framework Si/Al ratio (Taarit et al. 1994).

X-Ray Photoelectron Spectroscopy (XPS) is informative to determine if surface and bulk compositions are identical or not (Vedrine, 1992). It is based on energy distribution of electrons that are emitted from the catalyst due to the photoelectric effect. Although XPS is predominantly used for studying surface compositions and oxidation states, the technique also yield information on the dispersion of supported catalysts.

CHAPTER IV

EXPERIMENTAL STUDY

Na-ZSM-5 type zeolite samples were synthesized for different synthesis times, synthesis modes and with different hydrogel compositions. A synthesis work for K-ZSM-22 type zeolite was also carried out both in static and rotational mode. The work related to the effect of synthesis time and mode of stirring on ZSM-5 samples was carried out at Abo Akademi University. Synthesized zeolites were characterized, transformed to H-form catalysts and tested for 1-butene skeletal isomerization using a fixed bed reactor. Detailed description about the studies are given below.

4.1. SYNTHESIS OF Na-ZSM-5 ZEOLITES WITH VARIOUS SYNTHESIS TIMES AND MODE OF STIRRING

The chemicals used for the preparation of the synthesis gel is given in Table 4.1.

Table 4.1. Chemicals used for the synthesis of ZSM-5 zeolite samples.

Chemicals	Abo Akademi Unv.	Izmir Inst. of Tech.
Fumed silica	Aldrich, 99.80%	Sigma, 99.8%
$Al(OH)_3$	Aldrich 50-57% Al_2O_3	Merck, pure powder
NaOH	Merck, 99%	Sigma, >98.4%
TPABr	Fluka, >98%	Fluka, >98%

For the synthesis of Na-ZSM-5 zeolites with various synthesis times exactly the same hydrogel composition for each sample was used. The composition of the hydrogel was applied according to a recipe given in literature (Nicolaides, 1999). The detailed description of gel preparation is as follows:

Firstly three different solutions named, A, B and C, were prepared:

Solution A was prepared by adding 20.10 g fumed silica to 162.50 ml distilled water. Solution B was prepared by dissolving 4.48 g NaOH and 0.68 g $Al(OH)_3$ in 18.75 ml distilled water. The solution B was added to the solution A and mixed for 15 minutes. Then the solution C, prepared by dissolving 7.43 g of tetra-propyl-ammonium bromide (TPABr) in 75 ml of water, was added to the previous mixture. An additional amount of

110 ml of water was added after 15 minutes of agitation. After 15 minutes of agitation the gel was transferred to the autoclave.

The initial composition of the gel prepared was:
12.84 Na_2O : Al_2O_3 : 76.73 SiO_2 : 6.4 TPABr : 3962.6 H_2O

The initial gel composition was determined on the basis of following postulated equations:
$2NaOH = Na_2O + H_2O$ and $2Al(OH)_3 = Al_2O_3 + 3H_2O$

As the synthesis gel was prepared, it was filled into a Teflon lined autoclave. The reaction were either performed in static conditions or by rotating the autoclave through a shaft. At the end of the each synthesis time, the autoclave was taken out from the oven and cooled down by immersing into the cold water.

The sample collected from the autoclave was filtered and continuously washed with excess amount of distilled water. The cake allowed to dry in ambient medium and then dried in an oven at 110^{o}C for 24 hours.

An air-ventilated and temperature-programmable furnace was used for the calcination of the samples. The temperature of the furnace was increased from room temperature to 300^{o}C (in about 30 minutes) and allowed to stay at this temperature for 30 minutes, then it was heated to 540^{o}C with a heating rate of 6^{o}C/min and kept at this temperature for 8 hours. Finally, the temperature of the furnace was then slowly cooled down to room temperature.

The samples synthesized from the same hydrogel composition for various synthesis times and synthesis modes are given in Table 4.2.

The samples are labeled such that: Letter R and S denotes for the Rotational and Static synthesis modes respectively. Number preceding the letter (h) represents the synthesis time in hours.

Table 4.2. ZSM-5 samples synthesized of different synthesis time and mode of stirring.

Sample Label	Synthesis Time	SiO_2/Al_2O_3 Ratio	SiO_2/ TPABr Ratio	Variable Parameter
R-03h	3 hours	77	12	Synthesis Time
R-06h	6 hours	77	12	Synthesis Time
R-12h	12 hours	77	12	Synthesis Time
R-24h	24 hours	77	12	Synthesis Time
R-48h	48 hours	77	12	Synthesis Time
R-72h	72 hours	77	12	Synthesis Time
S-72h	72 hours	77	12	Synthesis Mode

The ZSM-5 zeolite catalysts synthesized for various synthesis times and mode of stirrings were tested for the transformation of n-butane to iso-butane in another study and reported elsewhere (Kumar et al, 2001).

4.2. SYNTHESIS OF Na-ZSM-5 ZEOLITES WITH DIFFERENT SiO_2/Al_2O_3 AND SiO_2/TPABr RATIOS

The hydrogel compositions for the samples employed were chosen according to a patent (Argauer et al, 1972).

The gel preparation, crystallization, filtration, washing, drying and calcination of these samples were carried out exactly the same as described for the samples synthesized for various synthesis times and mode of stirrings with an only exception of the hydrogel compositions. The zeolite samples synthesized with various SiO_2/Al_2O_3 ratio and TPABr content are given in Table 4.3. The samples are labeled such that: The two digit number (15, 30 or 70) denotes the initial SiO_2/Al_2O_3 ratio of the hydrogel. Number preceding the letter (D) represents the synthesis time in days. The codes (T), and (A) represents the sample synthesized with medium and low TPABr content respectively.

Table 4.3. ZSM-5 samples synthesized for various SiO_2/Al_2O_3 Ratio and TPABr content.

Sample Label	Synthesis Time	SiO_2/Al_2O_3 Ratio	SiO_2/ TPABr Ratio	Variable Parameter
S-15-4D	96 hours	15	3,3	Al_2O_3 Amount
S-30-4D	96 hours	30	3,3	Al_2O_3 Amount
S-70-4D	96 hours	70	3,3	Al_2O_3 Amount
S-30-2D	48 hours	30	3,3	TPABr Amount
S-30-2D-T	48 hours	30	5,5	TPABr Amount
S-30-2D-A	48 hours	30	12,5	TPABr Amount

4.3. PREPARATION OF H-ZSM-5 ZEOLITE CATALYSTS

All Na-ZSM-5 samples synthesized with various synthesis time, mode of stirrings and hydrogel composition were ion-exchanged with 1M NH_4Cl (Merck, 99.8%) solution for 48 hours at ambient temperature under continuos agitation. The steps followed for the preparation of H-ZSM-5 zeolites from Na-ZSM-5 is demonstrated in

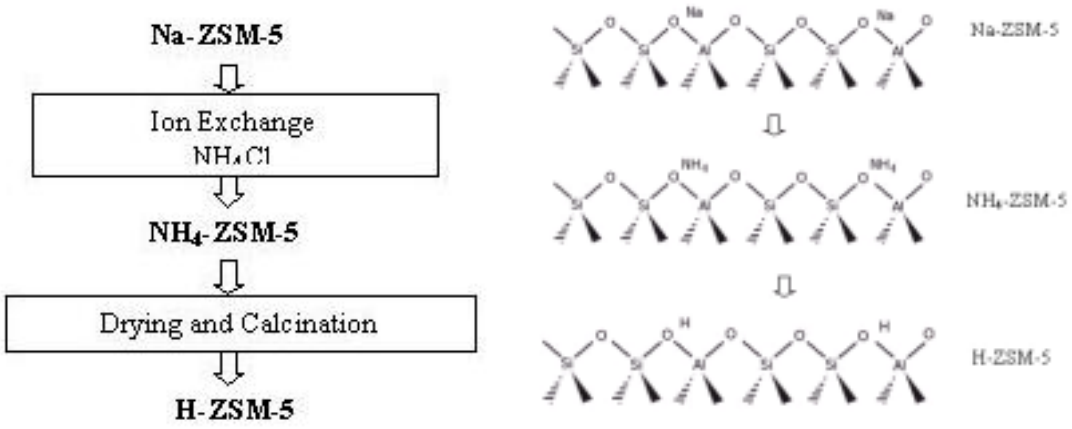

Figure 4.1. Steps followed for converting the Na-ZSM-5 samples to H-ZSM-5.

After ion exchange the zeolites were washed thoroughly until they are free of chloride ions. The samples were dried at 110^oC for 24 hours and slowly heated to 540^oC (6^oC/min) and calcined for 4 hours to remove NH_3 and to obtain the H-form zeolites.

Finally, in order to minimize internal diffusional limitations during the tests, the catalyst were sieved to achieve 125-250 μm (Byggningsbacka et al. 1998) agglomerates.

4.4. SYNTHESIS OF K-ZSM-22 ZEOLITE

The gel with the composition of 90 SiO_2: $Al_2(SO_4)_3$: 27 KOH: 27 1-6DAH: 3600H_2O was prepared by following the procedures reported previously (Valyocsik et al, 1990; Park, S.K. et al, 2000) which was done as follows:

Solution A was prepared by diluting Ludox (Aldrich, AS-40 40% wt. SiO_2) in 100 ml deionized water. Solution B was prepared by dissolving $Al_2(SO_4)_3.xH_2O$ (Aldrich, 98 %, x=14 –18) in 160 ml deionized water. 1,6-Diaminohexane (Fluka, >99 %) and KOH (Merck, pure) were added to solution B. After agitation of the mixture for 15 minutes, it was added to solution A. An agitation time of 30 minutes was applied for the final mixture.

The gel was filled into the Teflon lined autoclave and the synthesis was performed in both static and rotational modes at 150^oC for 4 days. The sample synthesized with rotational synthesis mode was labeled as R-TON and the samples synthesized in static mode was labeled as S-MFI. The calcination of these samples were performed at 540^oC for 16 hours with a heating rate of 6^oC/min.

These samples were also converted to H-form catalyst through consecutive ion-exchange, calcination and sieving procedures as described above for the ZSM-5 samples.

4.5. CHARACTERIZATION OF THE SAMPLES

The physico-chemical properties of each sample were identified by X-Ray Powder Diffraction, Scanning Electron Microscopy and the N_2 Adsorption-Desorption isotherms.

The crystalline structure of the samples were determined by means of X-ray powder diffractometers, Philips pw 1830 (Abo Akademi University) and Philips Xpert-Pro with CuKα radiation.

The adsorption isotherms and surface area calculations of the samples were determined by using nitrogen adsorption technique with Sorptomatic 1900, Carlo Erba Instruments (Abo Akademi University) and ASAP 2010 Micromeritics.

Scanning Electron Microscopy, Leica Cambridge Stereoscan 360 (Abo Akademi University) and Philips XL30 SFEG SEM were used for the identification of the particle sizes and morphologies of the samples.

The bulk SiO_2/Al_2O_3 ratios of some samples were determined by Varian-96 Inductively Coupled Plasma Atomic Emission Spectrometer (ICP-AES) with fusion dissolution method which is summarized below: 0.2 g of sample was mixed with 2 g of lithium tetraborate, then mixture was fused in furnace at 1000 ^oC for 45 minutes and allowed to cool. Formed glass bead was dissolved in 1.6 M HNO_3 solution on a magnetic stirrer. Solution was completed to 250 ml by ensuring 5 v/v % of 65 % HNO_3 and diluted if necessary.

Schimadzu TGA-51 was used for the thermal analyses.

4.6. CATALYST TESTING

A fixed bed reactor system illustrated in Figure 4.2. was constructed for the testing of catalysts for 1-butene skeletal isomerization reaction. The reaction system was composed of a quartz fixed bed tubular reactor (10 mm in diameter and 65 cm in length) heated with a tubular furnace. The reaction temperature was sensitively controlled with a thermocouple probe placed very close to the catalyst bed inside the reactor. The reactant 1-butene and the dilutant nitrogen were united and fed to the reactor after passing through the needle valves, mass flow controllers and check valves.

The packing of the catalyst was done as follows: initially a proper amount of quartz wool was placed inside the quartz reactor. On top of it, 0.2 g of quartz sand, 0,05 g catalysts and another 0.2 g of quartz sand was filled in the given order. Thus the catalyst was placed between two layers of quartz sands. After packing, the reactor was inserted inside the tubular furnace and connected to leak free gas line. Swagelock ultra torr fittings and bored through connectors were used for the leak free connection of the quartz reactor and the thermocouple.

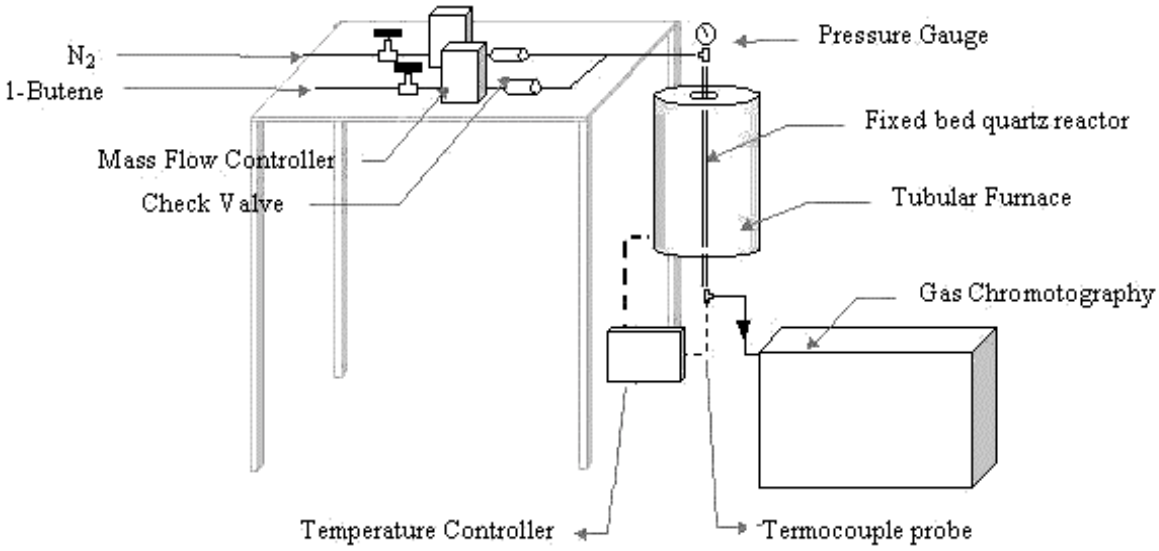

Figure 4.2. The experimental set-up constructed for testing the catalysts.

Before the reaction, the catalyst was heated to 440^{o}C in 60 minutes under 100 ml/min flow of nitrogen (99.99%) and maintained for additional 45 minutes at this temperature for activation and then cooled down to the reaction temperature. The reaction was started by flowing 1-butene (98%, 8 ml/min) and nitrogen (100ml/min) mixture to the reactor. Both nitrogen and 1-butene flow rates were sensitively adjusted through the flow controller.

To prevent any condensation, the line from reactor outlet to the injection port of gas chromatograph was externally heated and isolated. At time intervals the sampling loop system connected to the reactor outline was forwarded to the online gas chromatograph equipped with a Flame Ionization Detector (FID) and a fumed silica KCl column (GS-Alumina KCl, 50m x 0,53mm). A stepped heating and flow program was applied to the GC column for fine separation of all the reaction products.

CHAPTER V

RESULTS & DISCUSSIONS

5.1. INVESTIGATIONS ON CALCINATION TEMPERATURE

Thermal gravimetric analyses were performed to investigate the decomposition of the organic templates. TGA plot of a calcined and un-calcined ZSM-5 sample synthesized by using TPABr is presented in Figure 5.1. TGA plot of the calcined and un-calcined ZSM-22 sample synthesized by using 1,6-diaminohexane (1,6-DAH) is presented in Figure 5.2.

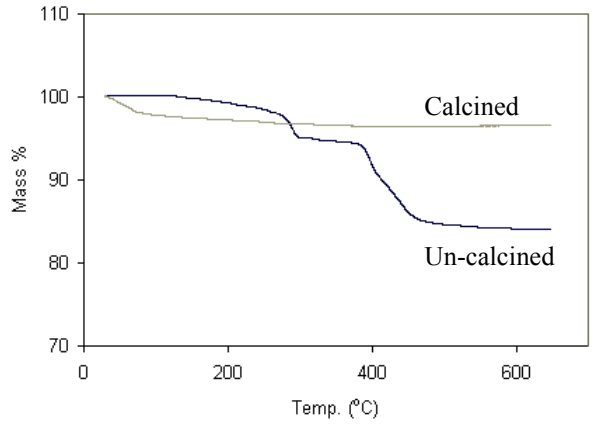

Figure 5.1. TGA plots of calcined and uncalcined ZSM-5 samples. Template used was tetrapropyl-ammonium bromide (heating rate: 5^{o}C/min).

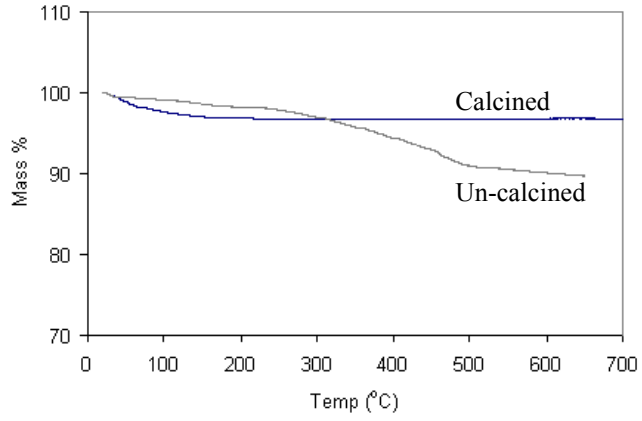

Figure 5.2. TGA plot of calcined and un-calcined ZSM-22 samples. Template used was 1,6-diaminohexane (heating rate: 5^{o}C/min).

The weight of the calcined ZSM-5 and ZSM-22 samples remained constant after the initial water evaporation from the samples. The weight of the uncalcined samples remained constant after 500^{o}C. So, these analyses confirmed the validity of the temperature program used for calcining the crystalline zeolite samples prepared.

5.2. INFLUENCE OF SYNTHESIS TIME AND SYNTHESIS MODE ON ZSM-5 SYNTHESIS

Zeolites were synthesized at synthesis times of 3, 6, 12, 24, 28 and 72 hours. The XRD patterns of the samples are given in Figure 5.3. The XRD patterns of the samples synthesized up to 6 h in rotational mode showed that, these samples were amorphous aluminosilicates. A small difference was recognized between samples synthesized for 3 h and 6 h. A small increase at the peak of $2\theta=23^{o}$ evidences the progressing nucleation and crystallization of the gel. On the contrary to the samples synthesized for up to 6 h, the sample synthesized for 12 to 72 hours (R-12h, R-24h, R-48h, R-72h) were highly crystalline. The positions of all peaks of these highly crystalline samples were the same and in accordance with those found in literature for the ZSM-5 structure (Kumar, 1996). So it was concluded that the resultant phase was ZSM-5 for the R-12h, R-24h, R-48h and R-72h samples. The differences in the XRD spectra of the samples synthesized for 6 and 12 hours were significant. The samples synthesized for 12 to 72 hours, showed similar X-ray diffraction patterns.

In Figure 5.3. XRD diffraction pattern of the sample synthesized for 72 hours in static synthesis mode is also given. This sample had the highest XRD intensity. Sample synthesized with the rotational mode had a lower XRD intensity. This could be because of enhanced dissolution due to the rotational mode.

Rotational Mode

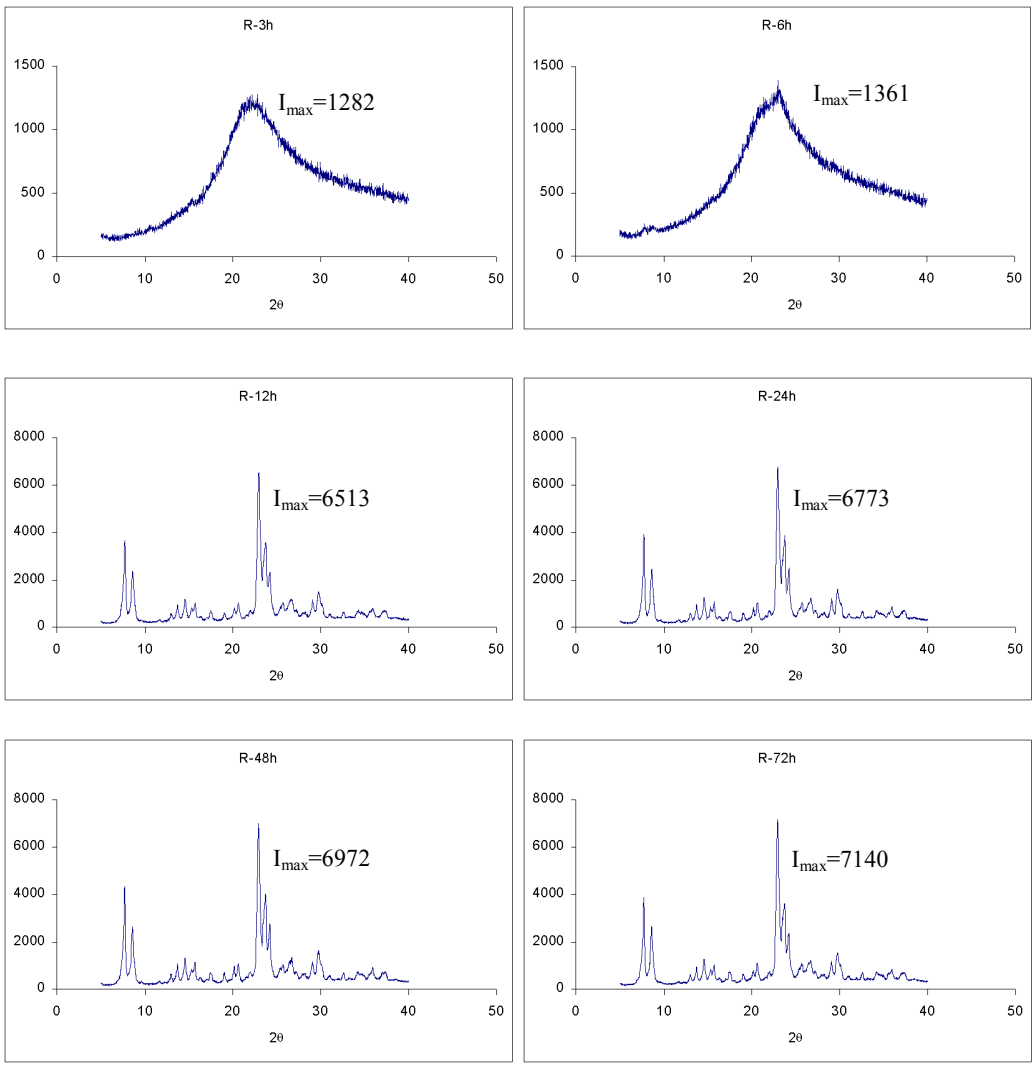

Static Mode

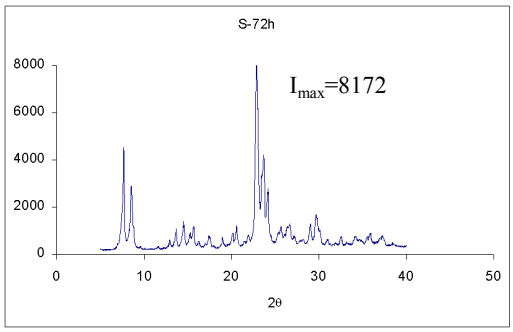

Figure 5.3. XRD paterns of R-03h, R-06h, R-12h, R24h, R-48h, R-72h and S-72h samples.

The percentage of crystallinity determination was estimated as commonly applied in literature (Hardenberg et al. 1992). Calculations are simply based on the intensity of the major peak, which do appear at $2\theta \cong 23^{o}$ and the sample with highest XRD intensity is referred as 100%. Therefore S-72h sample which had the highest XRD intensity among samples synthesized in Abo Akademi University was taken as the reference of 100% crystallinity. The percentage of crystallinity values were determined by using the formula:

$$\text{Crystallinity\%} = \frac{(\text{peak intensity of the product})}{(\text{peak intensity of the reference sample})} \times 100$$

The calculated percent crystallinity values of the samples synthesized with the rotational mode for different synthesis times are demonstrated in Figure 5.4.

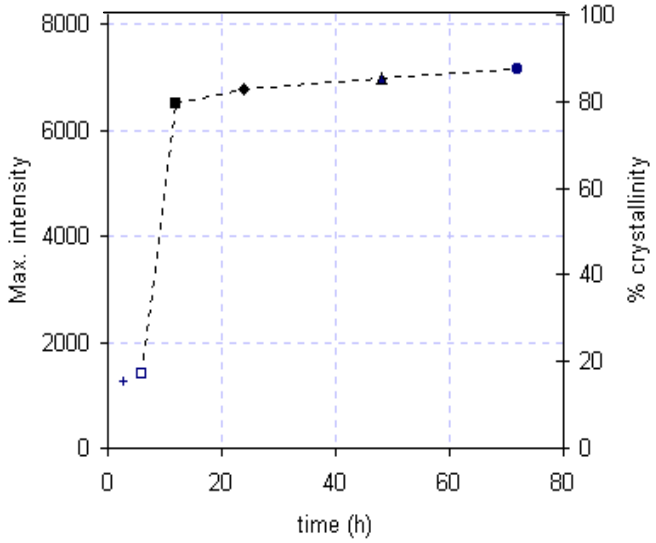

Figure 5.4. Percentage of crystallinity of R-3h (+), R-6h (□), R-12h (■), R-24h(◆), R-48h (▲) and R-72h (●) samples.

Crystallinity percentage sharply increased from 18 % to 83 % for the samples synthesized for 6 and 12 hours, respectively. However beyond 12 hours of synthesis time percentage crystallinity showed very slow increase.

The shape and the average particle sizes of the samples were determined from the Scanning Electron Micrographs and some images obtained are given in Figure 5.5.

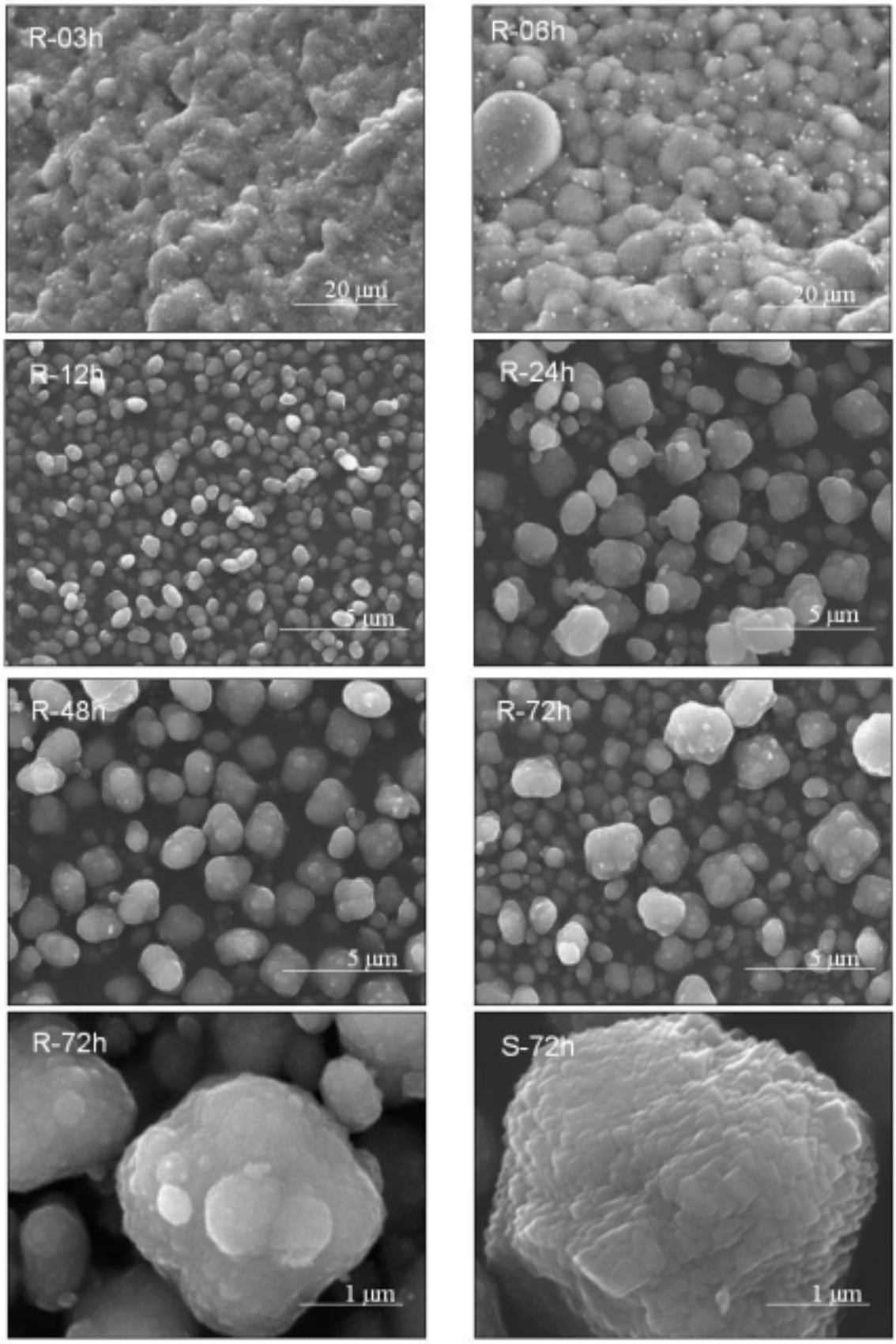

Figure 5.5. SEM images of R-03h, R-06h, R12h, R-24h, R-48h, R72h and S-72h samples.

The structure observed for 3h and 6h synthesis time were found to be amorphous agglomerates. Nucleates and small crystals formed at 6h was distinguishable by comparing the SEM micrographs of R-03h and R-06h. The particles that observed in SEM micrographs of R-12h, R-24h, R-48h and R-72h were either separated crystals and/or agglomerates of crystals. The particles were almost spherical.

The ZSM-5 zeolite crystals obtained when synthesis was carried out in rotational mode were smaller than those synthesized in static mode, for the same synthesis time. Similar observations were done by Asensi et al. 1998, where the zeolite synthesis procedure (static or rotating conditions) produced samples with different crystal sizes and larger particles were achieved with the static condition. The differences in the in the morphology with the synthesis mode might be caused by the enhanced dissolution of the crystals during rotation.

Average particle sizes of the samples were determined from SEM images by taking account the average diameter of at least 50 different particles. The average particle size values versus synthesis time are presented in Figure 5.6.

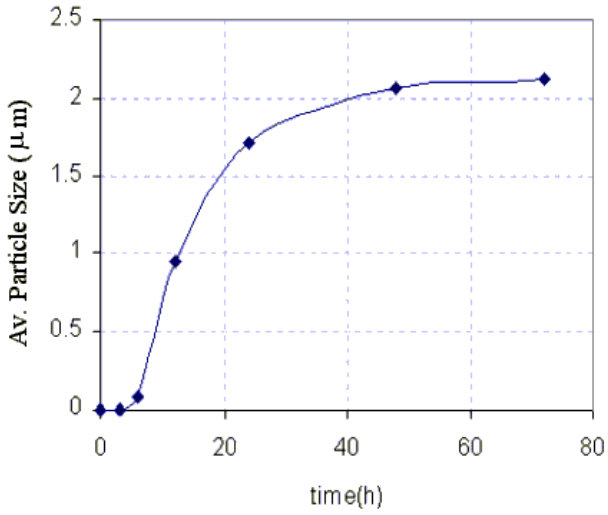

Figure 5.6. Average particlesizes for different synthesis times.

As shown in Figure 5.6. an increase in the particle size of the crystalline products was observed with increasing the crystallization time. When Figure 5.4. is compared with Figure 5.6. it was found that the change in the particle size and percentage

crystallinity for the synthesis time were not similar. The % crystallinity of the sample synthesized in 12 hours was almost same with the sample synthesized in 24 hours but this was not the same for the particle size. The average particle size of the sample synthesized in 24 hours was 1.7 μm whereas the average particle size of the sample synthesized in 12 hours was only 0.9 μm. This change may be due to the agglomeration of the small particles.

Figure 5.7. Represents the comparative adsorption/desorption plots of the R-03h, R-06h, R-12h, R-48h and R-72h samples.

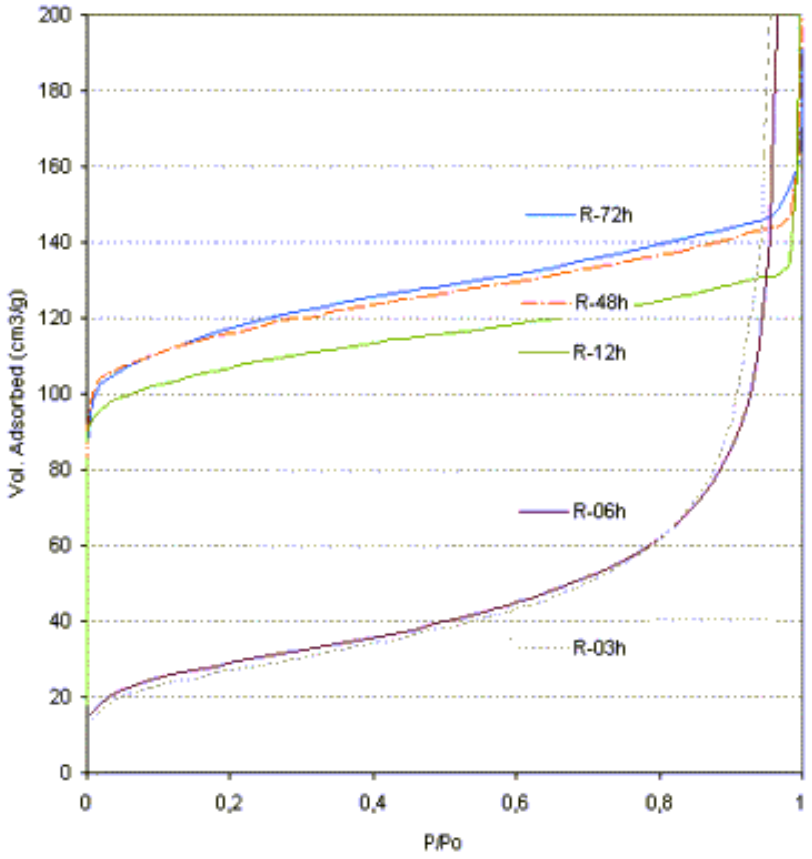

Figure 5.7. Adsorption curves of the samples synthesized by the rotational mode for various synthesis times.

The figure showed that the amorphous materials had very low adsorption capacities. On the other hand crystalline samples adsorbed much more N_2. An increase in the adsorption capacity was observed as the synthesis time was increased.

The specific surface areas of the samples were calculated by using the Dubinin Method and the results are presented in Table. 5.1.

Table 5.1. Specific surface area values calculated by the Dubinin Method for samples synthesized for different synthesis times.

Synthesis time (hour)	Specific Surface Area (m^2/g)
03	108.5
06	114.4
12	477.8
24	482.9
48	480.6
72	477.8

High surface areas were obtained for the high crystalline samples. The fully crystalline samples were found to have very close surface areas to each other, this clearly indicated that the particle size did not have a significant effect on the specific surface area of the samples.

5.2. INFLUENCE OF HYDROGEL COMPOSITION ON ZSM-5 SYNTHESIS

5.2.1. Influence of SiO_2/Al_2O_3 Ratio

Samples with initial SiO_2/Al_2O_3 ratios of 15, 30 and 70 were synthesized and labeled as 70-4D, 30-4D and 15-4D respectively. The bulk SiO_2/Al_2O_3 molar ratios of these samples were determined by ICP analysis and results are presented in Table 5.2.

Table 5.2. The bulk SiO_2/Al_2O_3 ratios of samples synthesized with various initial SiO_2/Al_2O_3 ratios.

Sample	Bulk SiO_2/Al_2O_3
Na-15-4D	21,7
Na-30-4D	32,1
Na-70-4D	81,6
H-15-4D	20,7
H-30-4D	35,8
H-70-4D	75,5

As expected, the Al content of the bulk samples increased as the Al content of the hydrogels were increased.

The XRD patterns and SEM images of the samples are presented in Figure 5.8. The XRD pattern of the sample 15-4D showed a slightly lower intensity than the 30-4D and 70-4D samples at $2\theta \approx 23.2^{o}$. This showed that high Al content had decreased the crystallization. This was an expected result since it is known that high Al content is not favored in the crystallization of ZSM-5. SEM images showed that there was not a significant difference between the particle sizes of the samples.

The adsorption-desorption isotherms of these samples are given in Figure 5.9. This figure showed that high Al content caused a decrease in the adsorption capacity of the samples. The sample with the highest SiO_2/Al_2O_3 ratio, i.e. the lowest Al content showed the highest adsorption capacity.

Textural properties determined by nitrogen adsorption analysis are presented in Table. 5.3. Specific surface area was found to increase by increasing the SiO_2/Al_2O_3 ratio of the samples. This could be due to the blockage of the pores with increased amount of cation that was incorporated in the structure to compensate the negative charge of the Al atoms or could be due to the lower degree of crystallization with higher Al content. Median pore diameters of the samples are found to be very close to each other and large enough for iso-butene diffusion.

Table 5.3 Textural properties of samples synthesized with different SiO_2/Al_2O_3 ratios.

Sample	D.A. Surface Area (m^2/g)	BET Surface Area (m^2/g)	H.K Median P.D. (Å)	Micropore Area (m^2/g)
H-15-4D	151,76	222,27	6,31	109,86
H-30-4D	441,46	294,84	6,45	157,20
H-70-4D	532,85	366,72	6,41	168,82

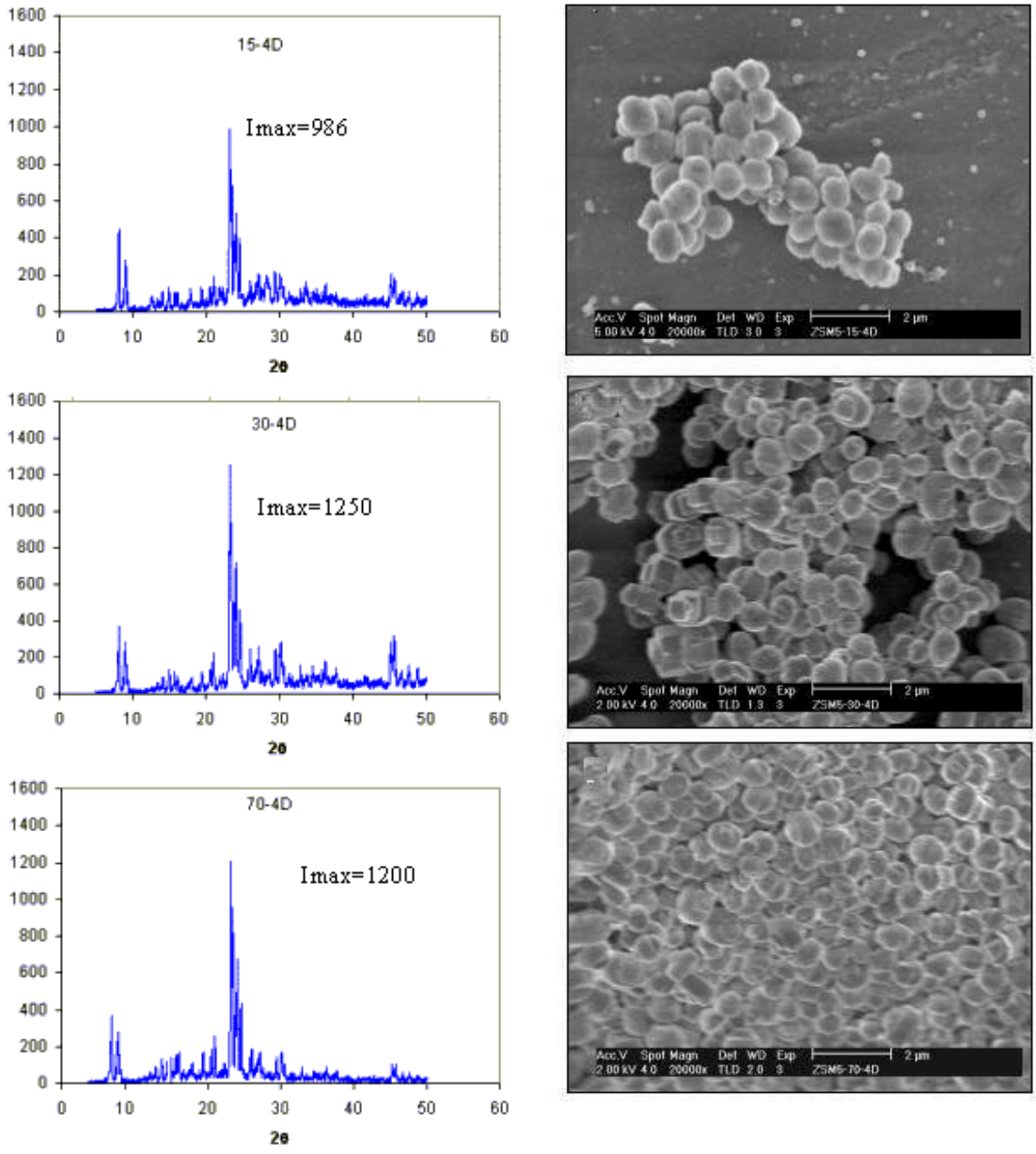

Figure 5.8. XRD pattern and SEM images of Na-15-4D (top), Na-30-4D (center), Na-70-4D (bottom).

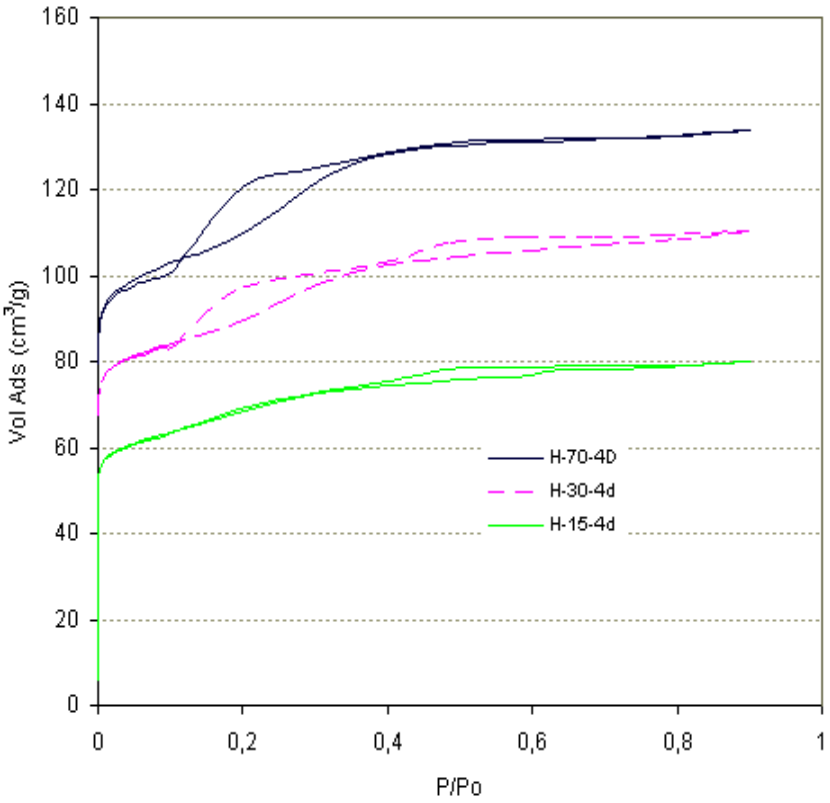

Figure 5.9. Adsorption/Desorption isotherms of the zeolite samples having various SiO_2/Al_2O_3 ratios.

5.2.2. Influence of SiO_2/TPABr Ratio

ZSM-5 samples synthesized with high, medium and low TPABr content were labeled as 30-2D (SiO_2/TPABr=3,3), 30-2D-T (SiO_2/TPABr=5,5) and 30-2D-A (SiO_2/TPABr =13,5).

The XRD patterns and SEM images of these samples are illustrated in Figure 5.10. The sample having the lowest TPABr content (30-2D-A) resulted in an amorphous phase. Organic template content of this sample was not sufficient to rearrange the Si and Al tetrahedrals to form a crystalline structure.

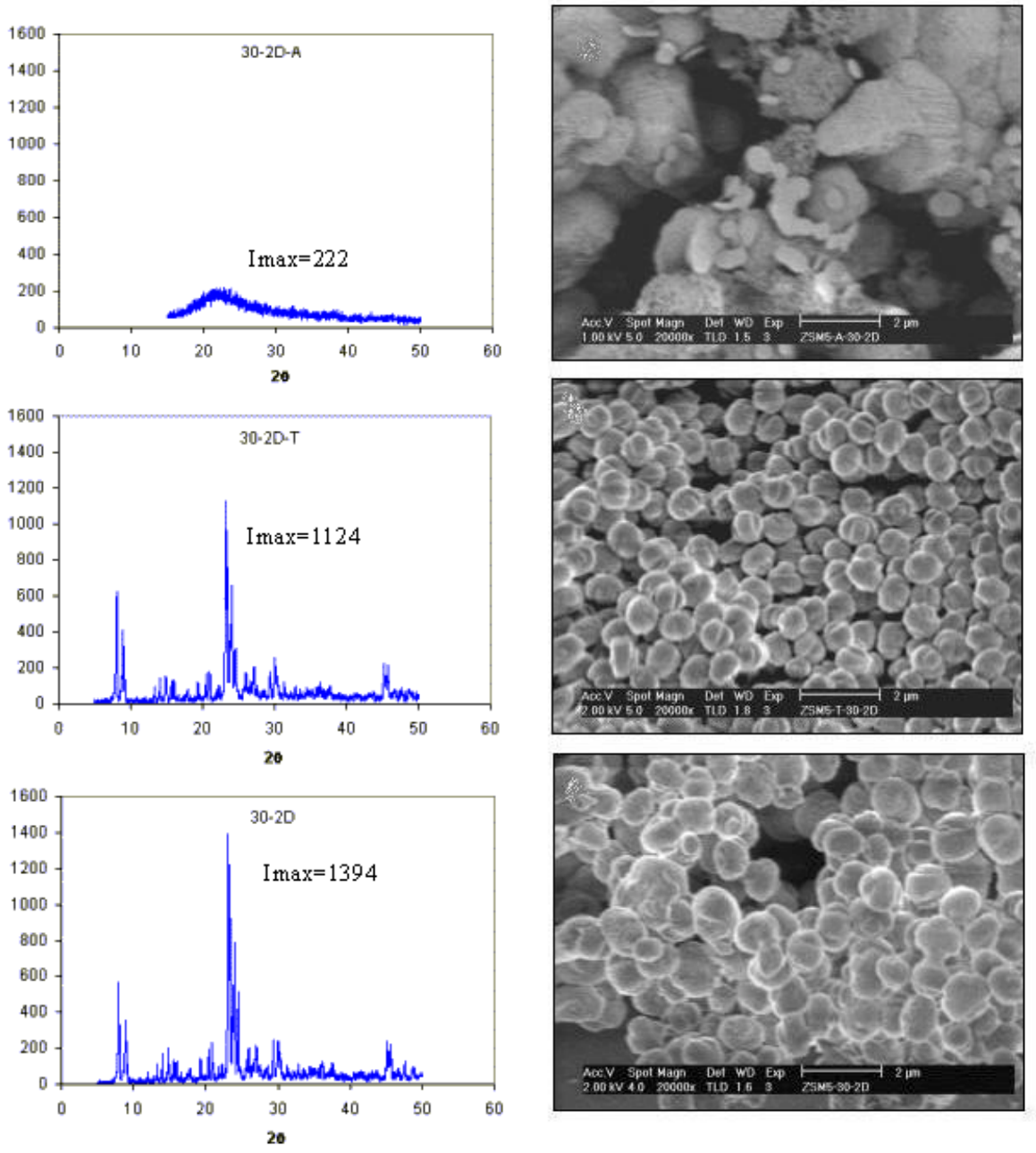

Figure 5.10. XRD pattern and SEM images of Na-30-2D-A (top), Na-30-2D-T (center) and Na-30-2D (bottom).

The sample having the highest TPABr content (30-2D) showed an increase in the crystallinity and in the particle size compared to the sample synthesized with moderate TPABr content. This showed that the organic template amount was very important for synthesizing highly crystalline samples. Howden 1982 also reported the quantity of template required in the syntesis has to be only moderately excess of the amount found in the final product and the reduced amount of template might cause significant decrease in the concentration of ZSM-5 crystals.

Adsorption and desorption isotherms of samples synthesized with high, medium and low TPABr content are shown in Figure 5.11.

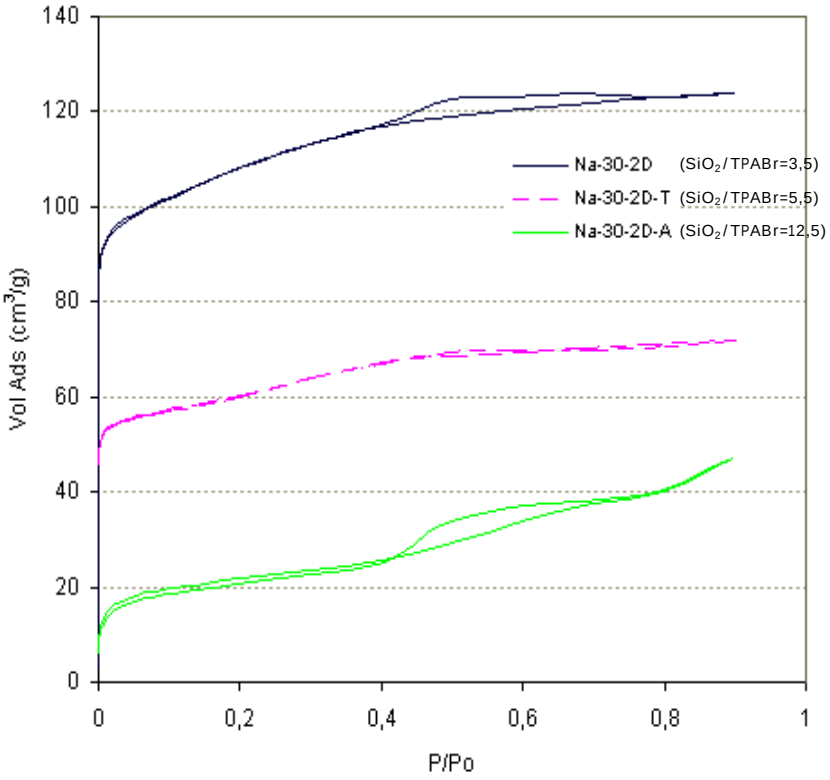

Figure 5.11. Adsorption/Desorption isotherms of the zeolite samples having various SiO_2/TPABr ratio.

Textural properties determined by the nitrogen adsorption analysis are presented in Table. 5.4. The specific surface area values showed an increase with increasing the TPABr content. This result was in accordance with the previous results obtained with XRD and SEM. Since an increase in the particle size and the crystallinity observed

with increase in TPABr content, an increase in the surface area and adsorption capacity was expected.

Table 5.4. Textural properties determined for samples synthesized with different initial SiO_2/TPABr ratio.

SiO_2/TPABr	D.A. Surface Area (m^2/g)	BET Surface Area (m^2/g)	H.K Median P.D. (Å)	Micropore Area (m^2/g)
3,5	454,62	285,10	6,37	165,53
5,5	305,94	193,32	6,42	124,87
12,5	98,18	71,74	6,32	27,76

Table 5.4. showed that the samples were having similar micropore diameters.

5.3. INFLUENCE OF SYNTHESIS MODE ON ZSM-22 SYNTHESIS

Experiments for the synthesis of ZSM-22 (or structurally called TON) was carried out in two different synthesis modes: Rotational and Static Mode. The XRD patterns of these samples are presented in Figure 5.12.

XRD results indicated that, completely two different morphological and crystallographic phases were achieved by using different synthesis modes. The location of the XRD peaks of the sample synthesized with the rotational mode (R-TON) were in accordance with the characteristic ZSM-22 peaks as given in the literature (Vartuili et al, 2000). From the nitrogen adsorption analysis, the BET surface and the median pore diameter of R-TON sample was found to be 110 m^2/g and 5,7 Å respectively.

On the other hand, XRD pattern of the sample synthesized with the static mode (S-MFI) showed that the resultant product was a highly crystalline ZSM-5 phase and the BET surface and the median pore diameter of this sample was found to be 296 m^2/g and 5,8 Å respectively. These results indicated that mode of stirring affects the crystal phase and morphology of the particles obtained. Asensi 1998 had also observed that some of ZSM-22 samples synthesized were having contamination of ZSM-5 phase, where this contamination was significantly greater for the samples synthesized in static

mode and on the other hand with the synthesis carried out under rotation, quite pure ZSM-22 crystallites except for a small impurity of ZSM-5 were obtained.

The SEM images of the R-TON sample are presented in Figure 5.13. The SEM images of R-TON sample proved the existence of a mixed field of different crystallographic phases. The major morphology of the ZSM-22 crystals was found to be needle shaped. The crystals of the minor phase were found to be very similar in shape of the previously synthesized ZSM-5 particles. This might supported an idea that the structure of the minor phase could be ZSM-5.

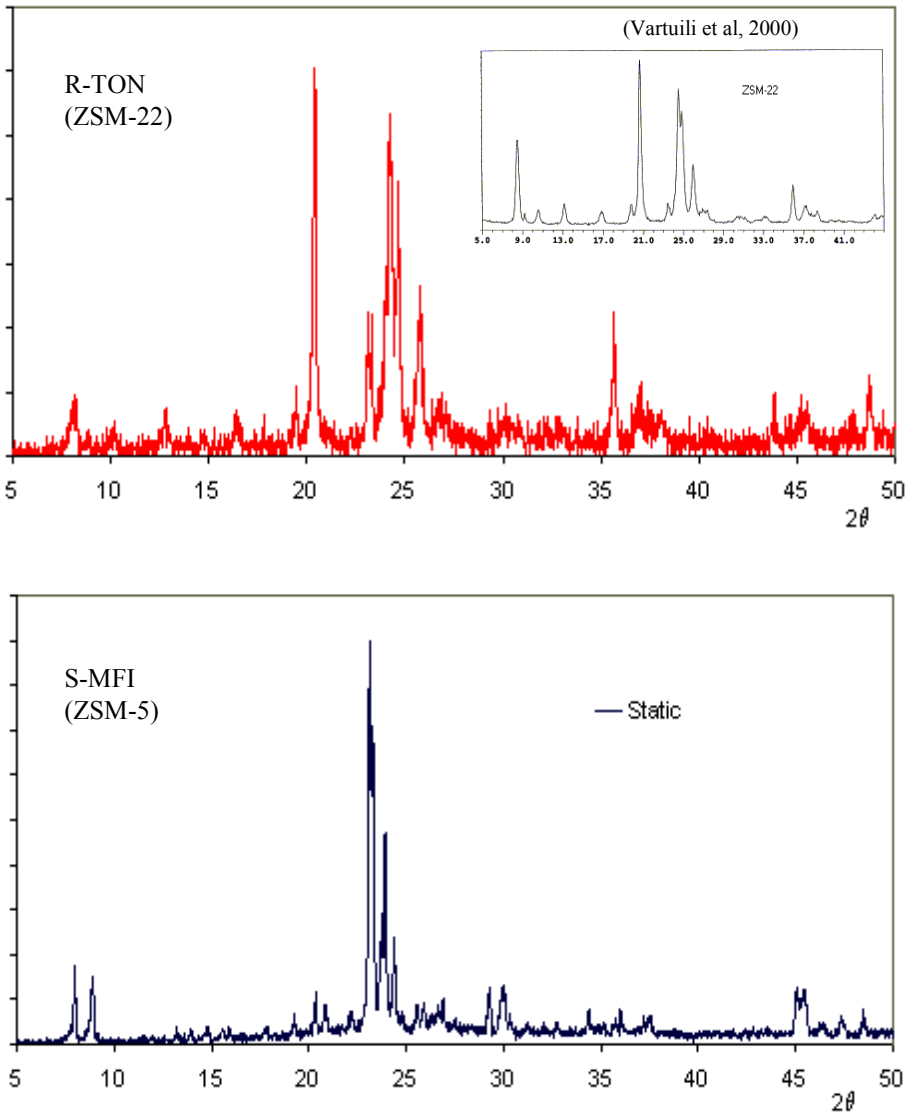

Figure 5.12. XRD patterns of the R-TON and S-MFI samples.

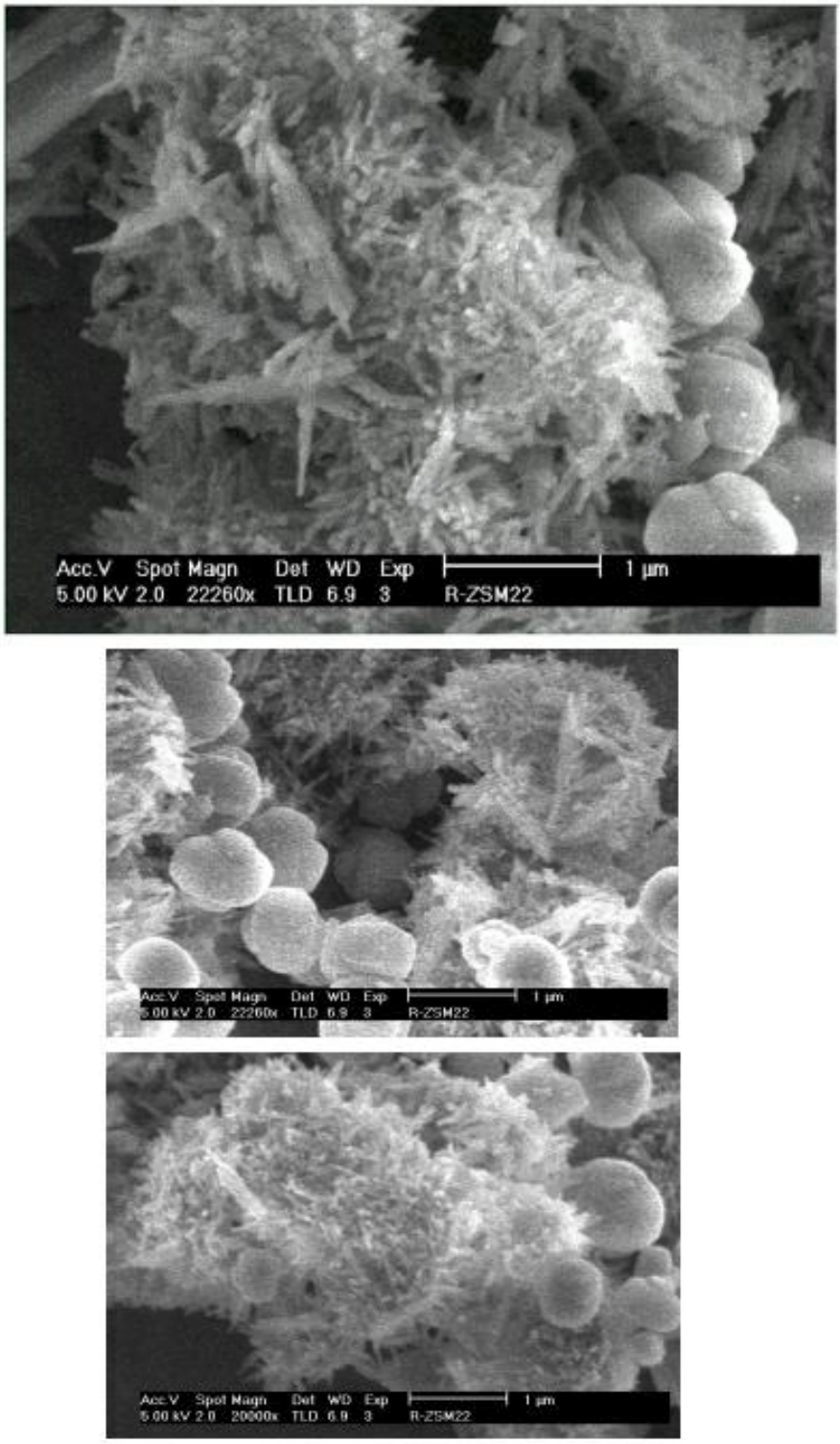

Figure 5.13. Scanning Electron Micrograph of the sample synthesized with the rotational mode (R-TON).

The particles of S-MFI sample, shown in Figure 5.14. were in shape of big agglomerates with sharp corners, having a morphology totally different from the previously synthesized ZSM-5 samples.

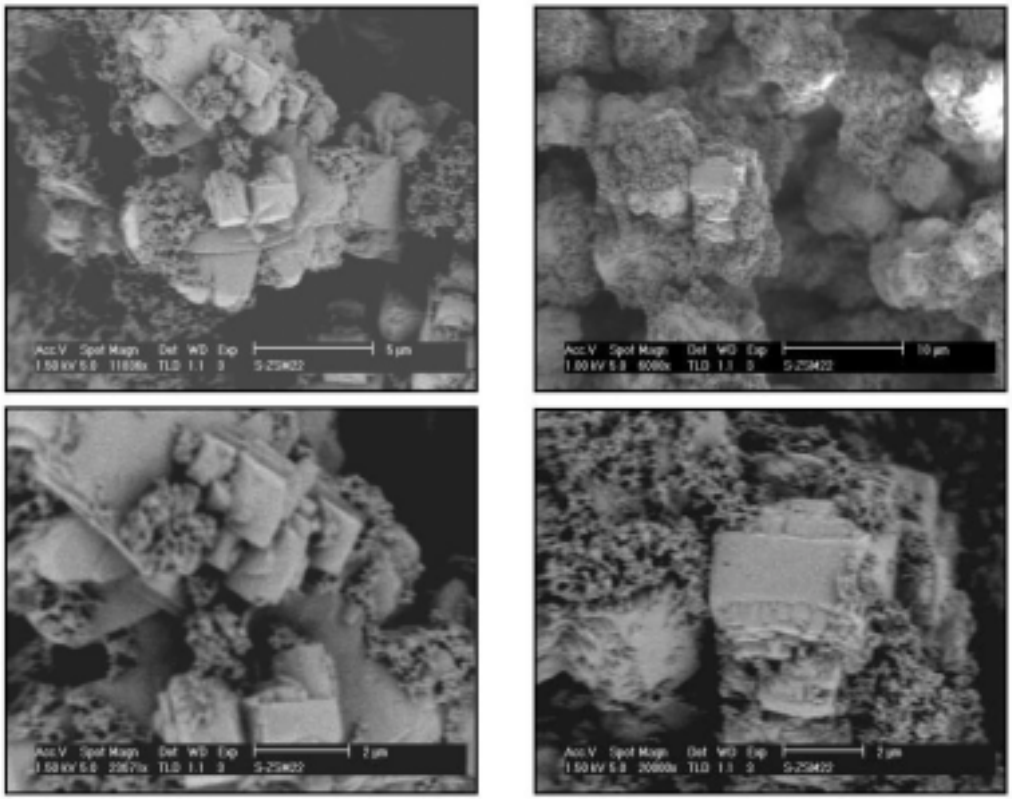

Figure 5.14. Scanning Electron Micrograph of the sample synthesized with the static mode (S-MFI).

5.4. CHARACTERIZATION OF THE COMMERCIAL ZSM-5 SAMPLE

A commercial H-ZSM-5 Zeolite catalysts (SiO_2/Al_2O_3=50) supplied from Sud Chemie was also characterized before testing in the reaction. The XRD pattern and SEM image is presented in Figure 5.15 and Figure 5.16.

The size of the commercial ZSM-5 particles was found to be very fine when compared to the synthesized ZSM-5 samples. The specific surface area of this catalyst was found to be 300 m^2/g.

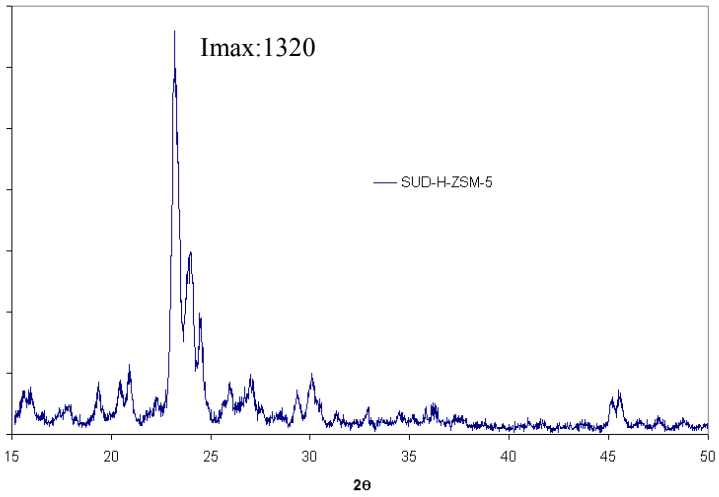

Figure 5.15. XRD pattern of commercial SUD-H-ZSM-5 sample.

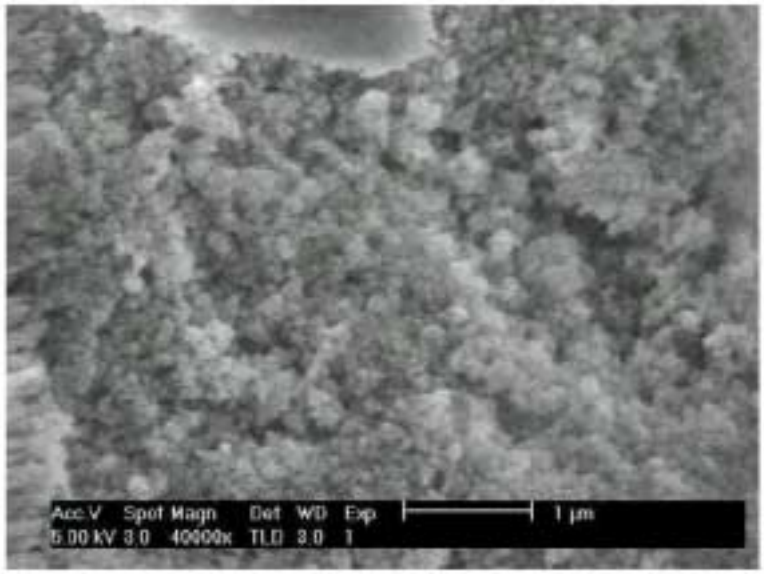

Figure 5.16. SEM image of the commercial SUD-H-ZSM-5 sample.

5.5. CATALYST TESTING

1-butene skeletal isomerization reaction were performed over H-15-4D, H-30-4D, H-70-4D, H-30-2D, H-30-2D-T, H-30-2D-A, H-S-MFI, H-R-TON and H-SUD-ZSM-5 catalyst samples. The reaction temperature and the Weight Hourly Space Velocity (WHSV) were determined by some preliminary studies as 440^{o}C and 22 h^{-1} respectively.

The best profile for column temperature and carrier gas (He) flow rate for a successful separation of the reaction products were investigated by preliminary studies. The change in column temperature and carrier gas flow rate during the gas chromatography analysis are illustrated in Figure 5.17.

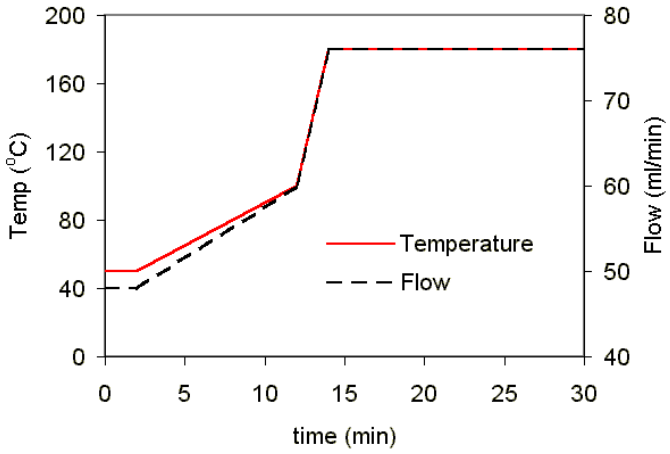

Figure 5.17. Column temperature and carrier gas flow rate during the gas chromatography analysis.

A sample gas chromatogram of the reaction products with this method is given in Figure 5.18.

Rapid double bond isomerization between 1-butene and 2-butene at the reaction temperature range causes equilibrium condition between 1-butene and 2-butenes (Gon Seo). So, trans-2 and cis-2 butene are regarded as reactants for the conversion calculation of 1-butene. The conversion of 1-butene is defined as the mass percent of reactant consumed. In addition, the selectivity to iso-butene is defined as the mass percent fraction of iso-butene to the consumed reactant and calculations were done as follows:

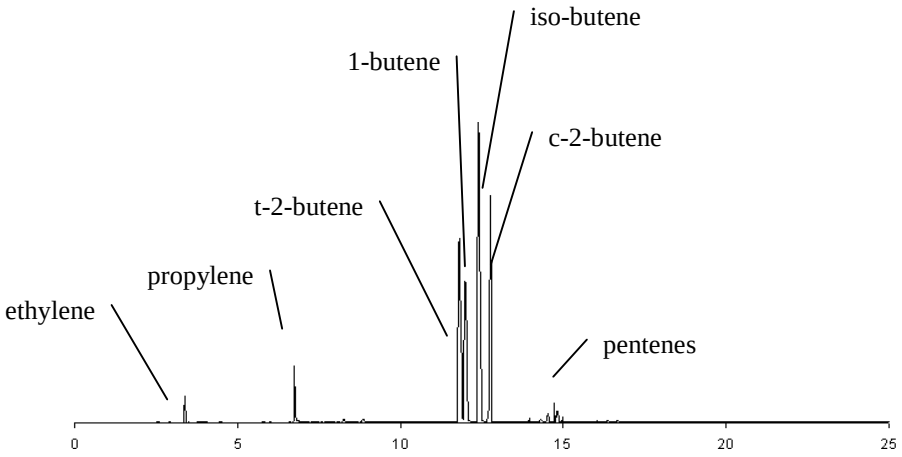

Figure 5.18. A sample Gas Chromatogram of the reaction products.

$$\%\ Conversion = \frac{(1-butene)_{in} - (n-butene)_{out}}{(1-butene)_{in}} \times 100$$

$$\%\ Yield\ of\ iso-butene = \frac{(iso-butene)_{out}}{(1-butene)_{in}} \times 100$$

$$\%\ Selectivity\ to\ iso-butene = \frac{(iso-butene)_{out}}{(1-butene)_{in} - (n-butene)_{out}} \times 100$$

The following relationship exists between conversion, yield, and selectivity:

$$Yield\ of\ iso-butene = conversion \times selectivity\ to\ iso-butene$$

5.5.1. Effect of SiO_2/Al_2O_3 Ratio on Catalytic Activity & Selectivity

The plot of conversion, selectivity to iso-butene and yield of iso-butene versus time on stream for the H-ZSM-5 catalysts synthesized for various SiO_2/Al_2O_3 ratio are given in Figure 5.19. According to Hardenberg et al. (1992), the catalytic activity (in terms of n-hexane cracking) of ZSM-5 zeolite catalysts were strongly depended on Al content. H-70-4D, H-30-4D and H-15-4D demonstrated almost the same catalytic conversion even though they were thought to have different acid site density (Figure 5.20.) Although the conversion of these catalysts were similar, selectivity to iso-butene was greatly influenced with Si/Al ratio. The catalysts, H-15-4D catalyst, which has the highest alumina content, showed very poor selectivity to iso-butene. H-70-4D and H-30-4D catalysts showed high selectivity to iso-butene and it was found that lowering the Al content resulted in a higher selectivity to iso-butene.

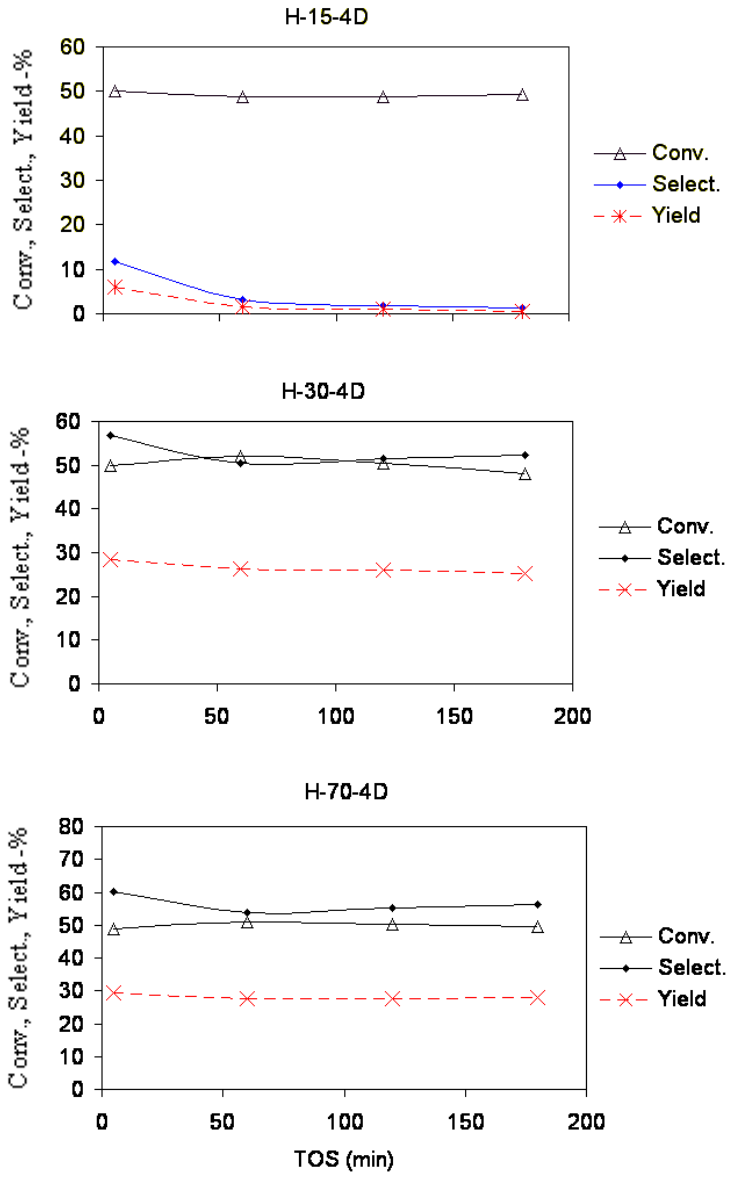

Figure 5.19. Conversion, yield of iso-butene and selectivity to iso-butene as a function of TOS over H-ZSM-5 zeolites synthesized with initial SiO_2/Al_2O_3 ratio of 15 (top), 30 (center) and 70 (bottom) at T= 440^{o}C, WHSV= 22 h^{-1}.

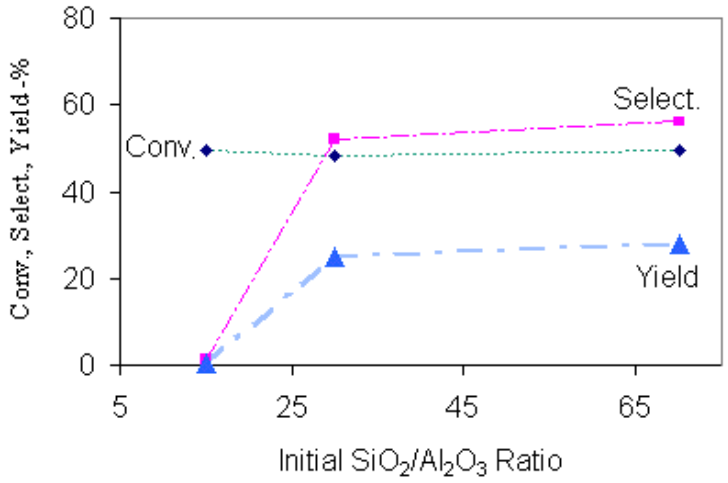

Figure 5.20. Percentage conversion, selectivity and yield for H-ZSM-5 samples having various initial SiO_2/Al_2O_3 ratios at T= 440°C, WHSV= 22 h^{-1}, TOS=3 h.

Mass distribution of the products after 3 hours on stream at 440°C over catalysts having various Si/Al ratio is given in Table. 5.5. 1-Butene was mainly converted to pentenes and propylene over the catalysts with the highest Al content. As the Si/Al ratio was increased more iso-butene was produced which was also in accordance with the observations of Asensi et al. (1998) where it was found that iso-butene selectivity increased when decreasing the acid site density, i.e. when increasing the Si/Al ratio.

These catalysts were having similar particle sizes but there existed an increase in the micropore area (increase in crystallinity) with increasing the Si/Al ratio, this could be another reason for having different selectivities to iso-butene.

Table 5.5. Product distribution obtained with H-ZSM-5 catalysts having various SiO_2/Al_2O_3 ratios at T= 440°C, WHSV= 22 h^{-1}, TOS=3 h.

	H-15-4D	H-30-4D	H-70-4D
Propylene	9,4	5,3	5,7
t-2-butene	15,1	17,3	17,2
1-Butene	22,6	19,8	18,8
Iso-butene	0,6	25,2	27,9
c-2-butene	13,0	14,8	14,4
1-pentene	17,0	6,0	4,4
Others	22,4	11,7	11,7

5.5.2. Effect of Crystallinity on Catalytic Activity & Selectivity

The plot of conversion, selectivity to iso-butene and yield of iso-butene versus time on stream for the H-ZSM-5 catalysts synthesized with various TPABr content are given in Figure 5.21. Since there was not enough crystalline formation in H-30-2D-A catalyst, this amorphous material was thought to be lack of both Bronsted and Lewis acid sites and as expected it demonstrated very low activity and almost no selectivity. As the TPABr content increases, i.e. the phase purity, the particle size and the surface area of zeolites were increased and therefore an enhancement in the conversion was observed as shown in Figure 5.22. It was concluded that the number of acid sites was increased with increase in the crystallinity. This result was in accordance with the findings of Hardenberg et al. 1982, that catalytic acitivity (in terms of n-hexane cracking) of the ZSM-5 catalyst samples increased with the crystallinity and similarly the amorphous catalyst showed extremely low activity.

Mass distribution of the products after 3 hours on stream at 440 ^{o}C over catalysts having various Si/Al ratio is given in Table. 5.6. Table 5.6. showed that 1-butene reacted increased with the TPABr content of the synthesis hydrogel, i.e. the crystallinity of the product.

Table 5.6. Product distribution obtained with H-ZSM-5 catalysts having various SiO_2/TPABr ratios at T= 440^{o}C, WHSV= 22 h^{-1}, TOS=3 h.

	H-30-2D	H-30-2D-T	H-30-2D-A
Propylene	4,4	2,9	3,4
t-2-butene	17,9	20,8	12,3
1-Butene	20,3	24,2	55,4
Iso-butene	28,2	24,0	0,4
c-2-butene	15,3	18,0	14,5
1-pentene	3,9	4,2	6,4
Others	10,0	5,9	7,6

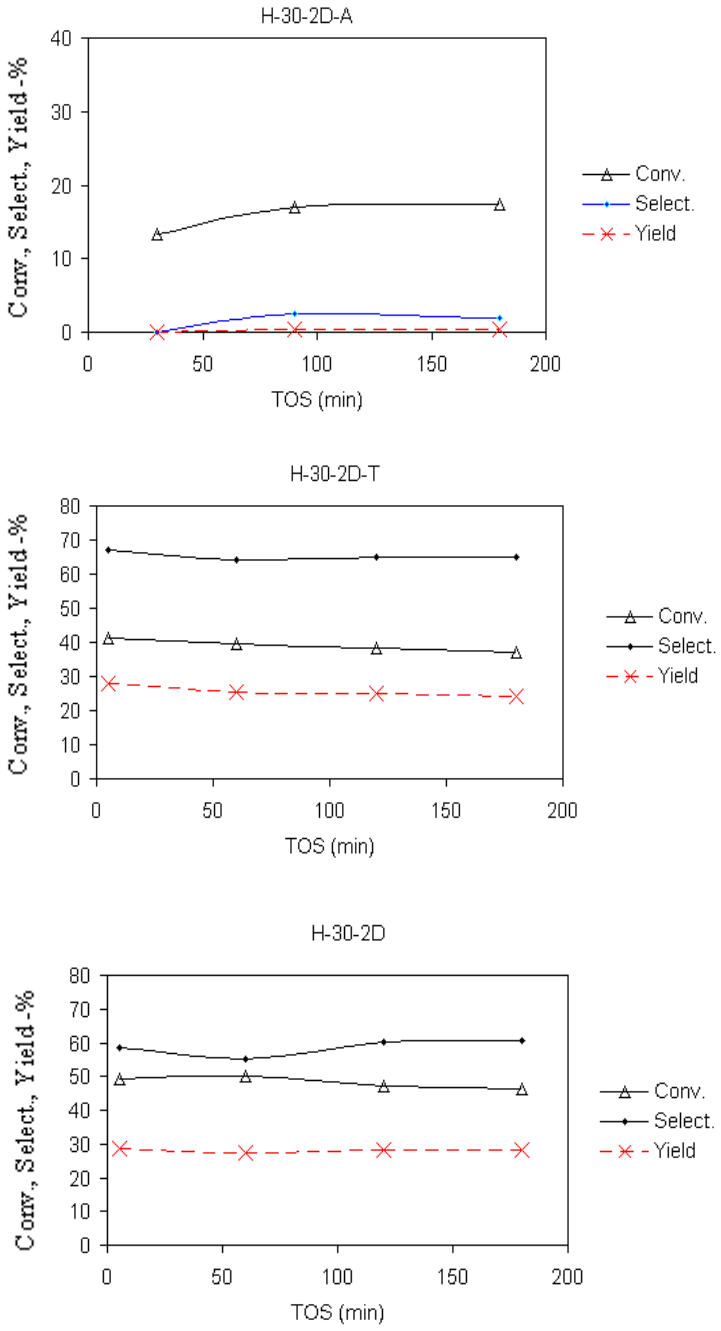

Figure 5.21. Conversion, yield of iso-butene and selectivity to iso-butene as a function of TOS over H-ZSM-5 zeolites synthesized with low (top), medium (center) and high (bottom) TPABr content at T= 440^{o}C, WHSV= 22 h^{-1}.

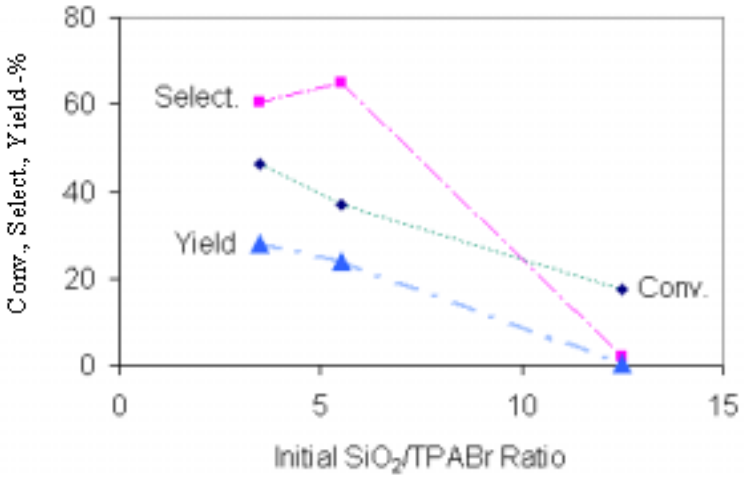

Figure 5.22. Percentage conversion, selectivity and yield for H-ZSM-5 samples having various initial SiO_2/TPABr ratios at T= 440^oC, WHSV= 22 h^{-1}, TOS=3 h.

5.5.3. Testing of H-R-TON and H-S-MFI Catalyst

The plot of conversion, selectivity to iso-butene and yield of iso-butene versus time on stream over H-R-TON and H-S-MFI are given in Figure 5.23. and Figure 5.24 respectively. H-R-TON sample showed 30% iso-butene yield up to 120 minutes on stream, but after that point catalyst showed a deactivation behavior.

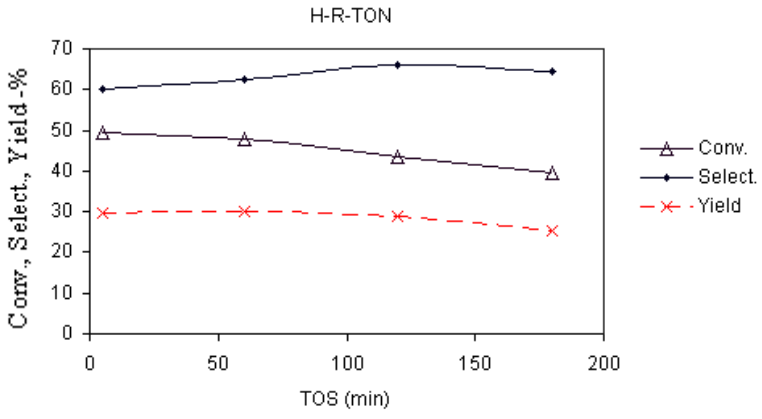

Figure 5.23. Conversion, yield of iso-butene and selectivity to iso-butene as a function of TOS over H-R-TON catalysts at T= 440^oC, WHSV= 22 h^{-1}.

The deactivation was more significant for the H-MFI sample with a very fast decrease in the iso-butene yield compared to other ZSM-5 catalysts. This catalyst showed poor catalytic activity and selectivity.

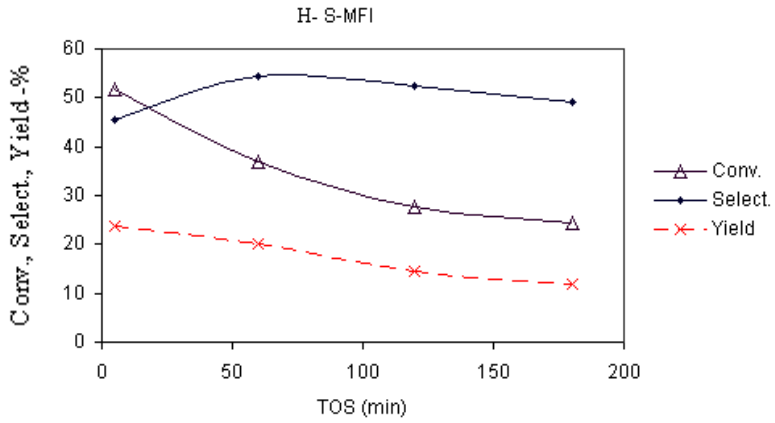

Figure 5.24. Conversion, yield of iso-butene and selectivity to iso-butene as a function of TOS H-S-MFI catalysts at T= 440^{o}C, WHSV= 22 h^{-1}.

5.5.4. Testing of H-Sud-ZSM-5 Catalysts

The plot of conversion, selectivity to iso-butene and yield of iso-butene versus time on stream over H-Sud-ZSM-5 is given in Figure 5.25. The commercial H-Sud-ZSM-5 catalyst although showed a very high conversion, the selectivity to iso-butene was very poor when compared to synthesized ZSM-5 catalysts. This catalyst was having very small particles, it was thought that most of the acid sites exist on the external surface and did not suppressed dimerization and by-product formation. It is very well known that shape selectivity of ZSM-5 zeolite is caused by its unique pore structure, therefore, the acid sites associated with the framework aluminium on the external surface of ZSM-5 crystallites do not contribute to shape selectivity. Smaller crystallites with larger surfaces may then be less selective than larger crystals (Namba et al. 1984).

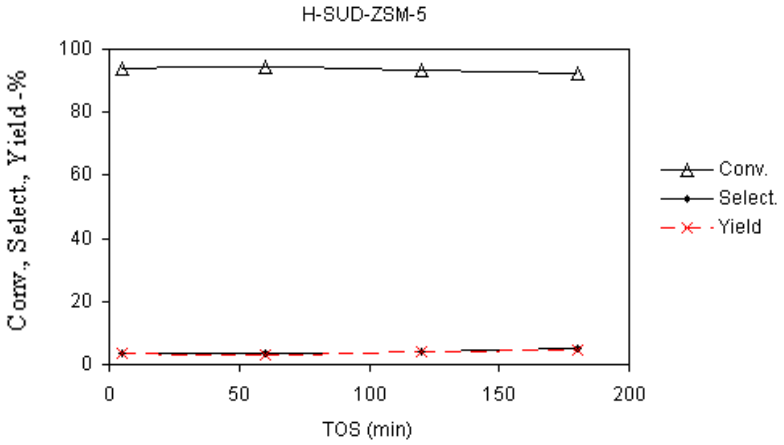

Figure 5.25. Conversion, yield of iso-butene and selectivity to iso-butene as a function of TOS over H-Sud-ZSM-5 catalysts at T= 440^{o}C, WHSV= 22 h^{-1}.

5.5.5. Effect of Time on Stream on Catalytic Activity and Selectivity

The reaction over H-30-2D catalyst at 375^{o}C and 22 h^{-1} WHSV was carried out for 24 hours on stream in order to determine the deactivation behavior of the catalyst. The results obtained are given in Figure 5.26.

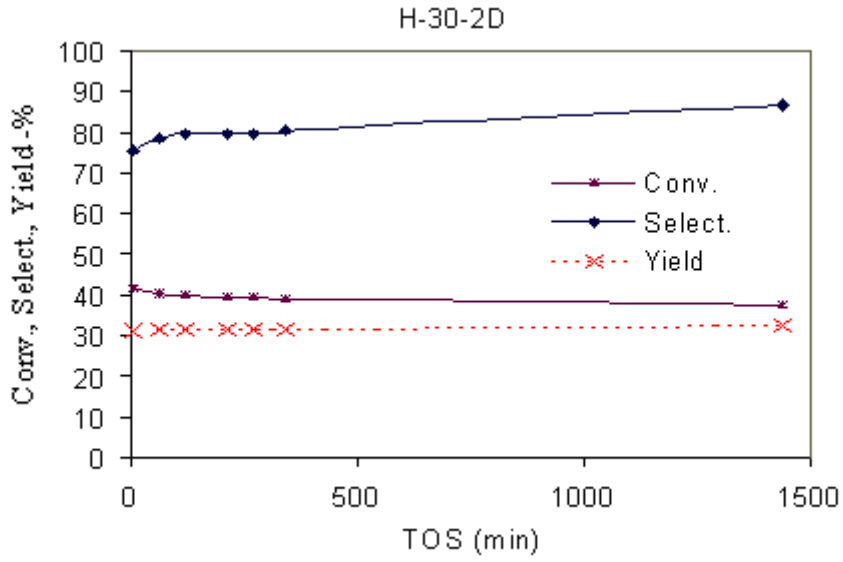

Figure 5.26. Conversion, yield of iso-butene and selectivity to iso-butene as a function of TOS over H-30-2D catalysts at T= 375^{o}C, WHSV= 22 h^{-1}.

It was found that the catalyst have a stable catalytic performance and iso-butene yield. The selectivity to iso-butene and iso-butene yield slight increased (from 32% to 33%) at 24 hours on stream . This result was attributed to several reasons by Houvicka et al. 1999:

1. Carbonaceous deposits poison preferentially the strongest acid sites, and the strong Bronsted acid sites are known to induce dimerization and thus can also induce the formation of by-products.
2. The outer surface of zeolite could be poisoned and thus the catalyst becomes by self-poising "better" shape selective. The shape selectivity can suppress the by product formation.
3. Carbonaceous deposits can eliminate irregularities in the molecular sieve structure.
4. Catalyst with deposits show slower conversion thus a lower extent of consecutive side reactions.

5.5.6. Effect of Reaction Temperature on Catalytic Activity & Selectivity

Skeletal isomerization of 1-butene to iso-butene is an exothermic reaction and therefore higher yield of iso-butene was expected at lower temperatures but unfortunately dimerization reactions are also favored at low temperatures (Byggningsbacka, 1999). So, H-30-2D catalyst which was found to be the most effective at 440^{o}C was also tested at 375^{o}C in order to investigate the effect of reaction temperature.

Figure 5.27. compares the conversion, selectivity to iso-butene and yield of iso-butene for two different reaction temperatures. At lowered reaction temperature, the conversion was decreased from 47% to 40%. On the other hand, the by product formation was suppressed and increased selectivity (from 60% to 79%) and increase in iso-butene yield (from 28% to 32%) was observed. The increment in the conversion by increasing the temperature was also observed by Byggningsbacka, 1999.

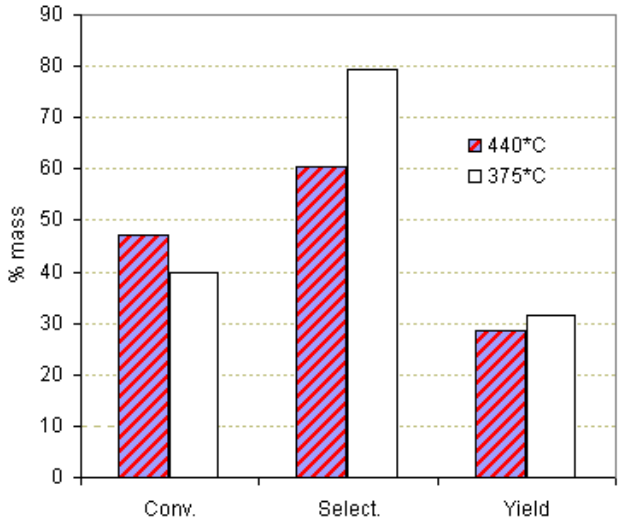

Figure 5.27. Conversion, yield of iso-butene and selectivity to iso-butene as a function of temperature at WHSV= 22 h^{-1} and TOS=3h.

5.5.6. Effect of WHSV on Catalytic Activity & Selectivity

According to Byggningsbacka 1999 iso-butene is reported to be the most reactive butene isomer in dimerization and higher selectivity to iso-butene was obtained at low levels of conversions when the yield of iso-butene was also low. Therefore, in order to obtain some selectivity to iso-butene, the WHSV of 1-butene needed to be adjusted so that the WHSV will be providing the equilibrium distribution among the butene isomers.

The amount of H-30-2D catalysts was doubled (0,1 g) so the WHSV was decreased in order to see the effect of WHSV. The reaction results for 11h^{-1} WHSV at 375^{o}C is given in Figure 5.28.

Figure 5.29. compares the conversion, selectivity to iso-butene and yield of iso-butene for two different WHSV values. Figure 5.28. showed that decreasing the WHSV had a positive effect on conversion. But, unfortunately, as the conversion increased, a decrease in the selectivity to iso-butene was observed and almost similar iso-butene

yields (32%) were achieved. This behavior was in accordance with the observations of Byggningsbacka 1999.

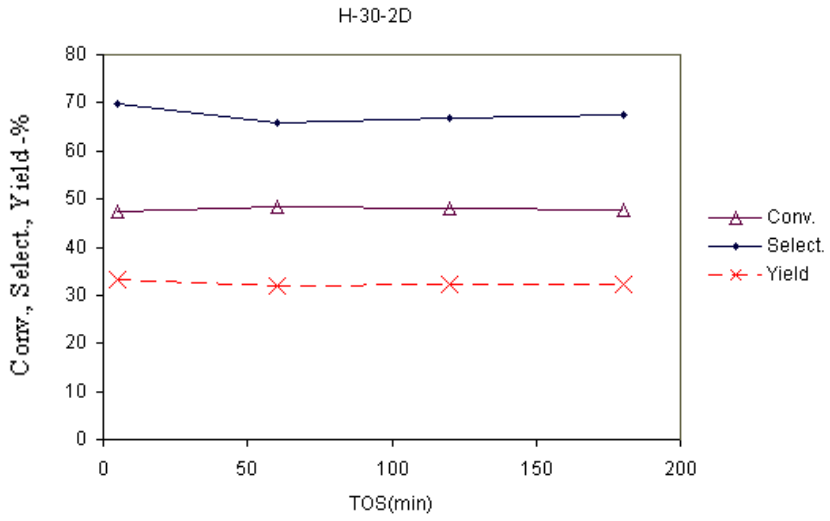

Figure 5.28. Conversion, yield of iso-butene and selectivity to iso-butene as a function of TOS over H-30-2D catalysts at 375°C and 11 h^{-1} WHSV.

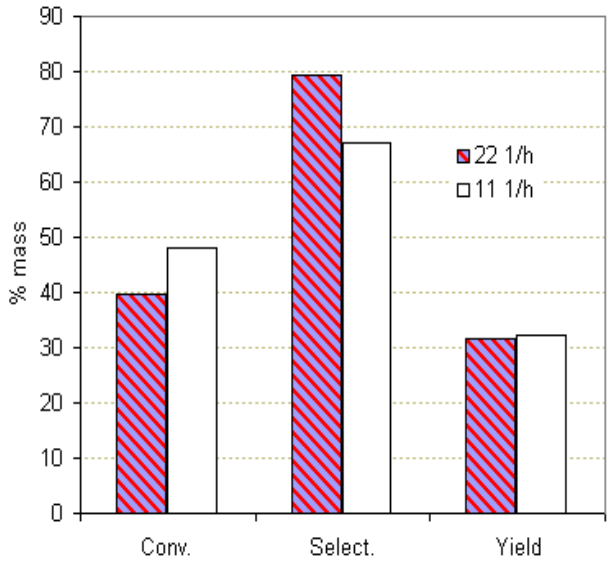

Figure 5.29. Conversion, yield of iso-butene and selectivity to iso-butene for different WHSV values at T=375°C and TOS=3h.

Thermodynamically determined relative concentration of iso-butene at 350^{o}C is reported to be 51% (Houzvicka et al. 1996) and even the best catalyst cannot escape the thermodynamics. When the total conversion passes over this value, the feed is more and more consumed by other reactions. As our knowledge, the highest iso-butene yield reported in the literature is 44% (350^{o}C, 48 h on stream, MHSV=2) (Nicolaides, 1999). Some high yields to iso-butene achieved by various researchers are given in comparison with the present study in Table 5.7. For achieving higher yield of iso-butene from prepared samples a further study is required where the reaction conditions (reaction temperature, WHSV, 1-butene partial pressure) can be optimized.

Table 5.7. Iso-butene yields achieved by various researchers.

Approx.Yield-%	Catalysts	Temp. (^{o}C)	Author(s)
33	ZSM-5	375	Present Study
41	SAPO-11	400	Yang et al 1999
44	ZSM-5	350	Nicolaides 1999
40	Fe-ZSM-22	350	Asensi et al. 1998
35	K-ZSM-22	500	Byggningsbacka et al. 1997
35	Mg-ZSM-22	450	Baeck and Lee 1998
35	ZSM-35	347	Wichterlova et al. 1999
30	Fe-ZSM-5	500	Houzvicka et al. 1998
40	ZSM-35	400	Canzires et al. 2000

CHAPTER V

CONCLUSIONS

Following conclusions were drawn for the synthesis and characterization studies:

Hydrogels that were reacted for insufficient synthesis times (3 and 6 hours) gave rise to amourphous aluminasilicate structure. The existence of the amorphous phase resulted in a low surface area. The increase in the synthesis time found to be effective in increasing the particle size of the ZSM-5 crystals. The rate of crystal growth decreased as the nutrition of the mother liquid is consumed for crystallization. Crystallinity remained almost constant for synthesis times above 12 hours but the particles became larger.

The particle morphology is effected by the stirring mode. Under strong basic conditions, the dissolution of the synthesis nutrition to the mother liquid was increased by the rotational synthesis mode. An increase in the particle size was also observed by increasing the TPABr content. Larger particles had longer diffusional paths and had higher surface areas. Al rich hydrogel resulted with slightly lower crystallinity and surface area. Lower Al content ZSM-5 crystals became larger more readily than aluminum rich ZSM-5.

Needle shaped ZSM-22 crystals were synthesized by the rotational synthesis mode. But the batch prepared for the synthesis of ZSM-22 zeolite and autoclaved in static mode produced a highly crystalline ZSM-5 phase. It was found that ZSM-5 can be still a favorable phase although a linear template, 1,6-diaminohexane was used. Therefore these results showed that for this gel composition and the synthesis conditions, a rotational system is required for achieving ZSM-22 phase.

Following conclusions were drawn for the catalyst testing study:

The catalyst sample having hydrogel SiO_2/Al_2O_3 ratio of 15 showed high activity but very low selectivity. In contrast under the same reaction conditions the samples having hydrogel SiO_2/Al_2O_3 ratio of 30 and 70 gave high selectivity and yield. This showed that the acidity of the catalysts were very important for high iso-butene selectivity. The

catalysts synthesized with the lowest crystallinity showed very low activity and selectivity to iso-butene because of the existence of amourph phase. The increased crystallinity resulted with higher iso-butene yield.

The highest crystalline sample with initial SiO_2/Al_2O_3 ratio 30 gave the highest yield to iso-butene among the all catalysts tested under the same reaction conditions. The yield of this catalyst was found to be increased by lowering the reaction temperature to 375^oC. This test was carried out for 24 hours and the catalyst showed stable catalytic activity with high performance. It was found that doubling the catalyst amount (WHSV=11 h^{-1}) at 375^oC increased the conversion but lowered the selectivity and same yield is achieved.

REFERENCES

Argauer, R. J. & Landolt,, G. R. U.S. Patent No: 3,702,886 : 1972.

Asensi, M. A.; Corma, A.; Martínez, A.; Derewinski, M.; Krysciak, J.; Tamhankar, S.S; "Isomorphous substitution in ZSM-22 zeolite. The role of zeolite acidity and crystal size during the skeletal isomerization of n-butene" Applied Catalysis A: General 174 (1998) 163-175

Baeck, S.H.; Lee, W.Y.; "Dealumination of Mg-ZSM-22 and its use in the skeletal isomerization of 1-butene to iso-butene" Applied Catalysis A: General 168 (1998) 171-177

Bhatia, S., Zeolite Catalysis: Principles and Applications, CRC Press, Inc. 2000, Florida

Breck, D.W., Zeolites Molecular Sieves: Structure, Chemistry and Use, Wiley, NY, 1974

Byggningsbacka R.; Lindfors, L.E.; Kumar N.; "Catalytic Activity of ZSM-22 Zeolites in the Skeletal Isomerization of 1-Butene" Ind. and Eng. Chem Res. 1997, 36, 2990

Byggningsbacka R.; Kumar, N.; Lindfors, L.E.; "Comparative Study of the Catalytic Properties of ZSM-22 and ZSM-35/Ferrierite Zeolites in the Skeletal Isomerization of 1-Butene" Journal of Catalysis 178, (1998) 611-620

Byggningsbacka R.; "Transformation of Light Hydrocarbons over Zeolite Catalyst" Doctoral Thesis, Abo Akademi University 1999.

Cañizares, P.; Lucas, de A.; Dorado, F. & Pérez, D.; "Effect of zeolite pore geometry on isomerization of n-butane" Applied Catalysis A: General 2000, 190:1-2:233-239

Cejka, J.; Wichterlová, B.; Sarv, P.; "Extent of monomolecular and bimolecular mechanism in n-butene skeletal isomerization to isobutene over molecular sieves" Applied Catalysis A: General 1999, 179:1-2:217-222

Collignon, F.; Mariani, M.; Moreno, S.; Remy, M.; Poncelet, G.; "Gas Phase Synthesis of MTBE from Methanol and Isobutene over Dealuminated Zeolites" Journal of Catalysis, Vol. 166, No. 1, Feb 1997, pp. 53-66

Clifton, R. A.; Natural & Synthtic Zeolites, Bureau of Mines Information Circular/1987 U.S. Department of The Interior.

Davis M. E.; "Zeolite-based catalysts for chemical synthesis" Microporous and Mesoporous Materials 21 (1998) 173-182

Falnigen, M.; "Zeolites and Molecular Sieves An Historical Perspective" In: Introduction To Zeolite Science and Practice H.van Bekkum, E.M. Flanigen, J.C: Jansen Elsevier Science Publishers B.V. 1991

Guisnet, M.; Magnoux, P.; "Deactivation of zeolites by coking, Prevention of deactivation and regeneration" : In: Zeolite Microporous Solids: Synthesis, Structure and Reactivity; E. G. Derouane, F. Lemos et al. Kluwer Academic Publishers, 1992. Netherlands.

Hardenberg T.A.J.; Mertens, L.; Mesman, P.; Muller, H.C.; Nicolaides, C.P.; "A catalytic method for the quantitative evaluation of crystallinities of ZSM-5 zeolite preparation" Zeolites, v.12 (1992) 685-689

Hindle S.; Transfer report Aug. 1997 Dept of Chem. Manchester Un.
(source: http:\\mch3w.ch.man.uk.\theory\staff\students\mbdtssh\trans\zeolites.html)

Howden, M. G.; "The Role of the TPA Template In the Synthesis of ZSM-5" Council for Scientific and Industrial Research, Pretoria, S.Africa.1982

van Hooff, J.H.C.; Roelofsen, J.W.; "Techniques of Zeolite Characterization" In: Introduction to Zeolite Science and Practice, H.van Bekkum, E.M. Flanigen, J.C. Jansen (Eds)Elsevier Science Publishers B.V. , 1991

Houzvicka, J.; Diefenbach, O.; Ponec, V.; "The Role of Bimolecular Mechanism in the Skeletal Isomerisation of n-Butene to Isobutene" Journal of Catalysis, Vol. 164, No. 2, Dec 1996, pp. 288-300

Houzvicka, J.; Hansildaar, S.; Ponec, V.; "The Shape Selectivity in the Skeletal Isomerisation of n-Butene to Isobutene", Journal of Catalysis, Vol. 167, No. 1, Apr 1997, pp. 273-278

Houzvicka, J.; Nienhuis, J.G.; Ponec, V.; "The role of the acid strength of the catalysts in the skeletal isomerisation of n-butene" Applied Catalysis A: General 1998, 174:1-2:207-212

Houzvicka, J.; Hansildaar, S.; Nienhuis, J.G.; Ponec, V.; " The role of deposits in butene isomerization" Applied Catalysis A: General 176 (1999) 83-89

Hölderich, W.F.; Bekkum, H.V.; "Zeolites in Inorganic Synthesis"; In: Introduction To Zeolite Science and Practice H.van Bekkum, E.M. Flanigen, J.C: Jansen Elsevier Science Publishers B.V. 1991.

Imelik, B.; Vedrine, J. C (Eds).; Catalyst Characterization, Physical Techniques for Solid Materials, 1994 Plenum Press, NY & London

Kumar, N.; "Synthesis, modification and application of high silica zeolite catalysts in the transformation of light hydrocarbons to aromatic hydrocarbons", Doctoral Thesis, Abo Akademi University 1996.

Kumar, N.; Nieminen, V.; Demirkan, K.; Salmi, T.; Murzin, D. Yu.; Laine, E.; "Effect of Synthesis Time and Mode of Stirring on Physico-Chemical and Catalytic Properties of ZSM-5 Zeolite in Isomerization of n-Butane to Iso-Butane" Proceedings of the 5th EuropaCat Conference, Limerick, Irleand, 2001, in press

Meisel, S.; Multifarious Uses of Synthetic Zeolites, Eur. Chem. News, v.42, Nov. 1984, pp 22, 27

Millini, R. "Application of modelling in zeolite science" Catalysis Today 41 (1998) 41-51.

Moulijn, J. A.; Sheldon, R.A.; Bekkum, H.V. and Leeuwen, P.W.N.M. "Catalytic processes in Industry": In: Catalysis, An Integrated Approach to Homogenous, Heterogenous and Industrial Catalysis, (Eds) J.A. Moulijn, P.W.N.M. van Leeuwen, R.A. van Santen Elsevier 1993

Moscou, L.; "The Zeolite Scene"; In: Introduction to Zeolite Science and Practice H.van Bekkum, E.M. Flanigen, J.C. Jansen (Eds) Elsevier Science Publishers B.V. , 1991.

Namba, S.; Inaka.; A.; Yashima, T.; " Effect of selective removal of aluminium from external surfaces of H-ZSM-5 zeolite on shape selectivity" Zeolites, 1986, v.6, 107

Nicolaides, C.P.; "A novel family of solid acid catalysts: substantially amorphous or partially crystalline zeolitic materials" Applied Catalysis A: General 1999, 185:2:211-217

Nikolopoulos, A.A.; Kogelbauer, A.; Goodwin, J. G.; Marcelin, Jr., G.; "Gas Phase Synthesis of MTBE on Triflic-Acid-Modified Zeolites" Journal of Catalysis, Vol. 158, No. 1, Jan 1996, pp. 76-82

Niemantsverdriet, J.W.; "Catalyst Characterization With Spectroscopic Techniques" In: Catalysis, An Integrated Approach to Homogenous, Heterogenous and Industrial Catalysis, (Eds) J.A. Moulijn, P.W.N.M. van Leeuwen, R.A. van Santen Elsevier 1993.

Ohayon, D.; Mao, R.L.V. et al, "Methods of pore size engineering in ZSM-5 Zeolite" Applied Catalysis A: General. 217 (2001) 241-251

Park, K.C.; Ihm, S.K.; "Comparison of Pt/zeolite catalyst for n-hexadecane hydroisomerization", Applied Catalysis A: General 203 (2000) 201-209

Rollmann, L.D.; "Synthesis of Zeolites, An Overview" In: Zeolites: Science and Technology, F.R. Riberio, A.E. Rodrigues, L.D. Rollmann, C. Naccache, Martinus Nijhoff Publishers, The Netherlands, 1984).

Seo, G., Park, S.-H., Kim, J.-H.; The reversible skeletal isomerization between n-butenes and iso-butene over solid acid catalysts" Catalysis Today 44 (1998) 215-222

Sherman, J.D: "Synthetic zeolites and other microporous oxide molecular sieves" Proc. Natl. Acad. Sci. USA, Vol96, pp.3471-3478, 1999
(source: www.nap.edu/openbook/0309064260/html/3471.html)

Simon, M.W.; Suib, S.L.; Oyoung, C.L.; "Synthesis and Characterization of ZSM-22 Zeolites and Their Catalytic Behavior in 1-Butene Isomerization Reactions" Journal of Catalysis, Vol. 147, No. 2, Jun 1994, pp. 484-493

Szostak, R. Handbook of Molecular Sieves; Van Nostrand, NY, 1992

Taarit, Y.B.; Fraissard, J.; In: Catalyst Characterization, Physical Techniques for Solid Materials, Imelik, B.; Vedrine, J. C (Eds). 1994 Plenum Press, NY & London

Thompson, R.W.; In: Molecular Sieves Science & Technology, H.Karge, J. Weitkamp (Eds) 1998 Springer.

Valyocsik, E.W.; Pa, Y.; United States Patent no:4,902,406 : 1990

Vartuli, J.C.; Roth, W.J., Beck, J.S., McCullen, S.B.; Kresge, C.T.; In: Molecular Sieves Science & Technology, H.Karge, J. Weitkamp (Eds) 1998 Springer.

Vartuli J.,C.; Kennedy G., J.; Yoon B.,A.; Malek A.; "Zeolite Synthesis using diamined: evidence for in situ directing agent modification" Microporous Materials, Vol. 38 (2000) 247-254

Vedrine, J.Q.; "General overview of the characterization of zeolites" In: Zeolite Microporous Solids: Synthesis, Structure and Reactivity; E. G. Derouane, F. Lemos et al. Kluwer Academic Publishers, 1992. Netherlands.

Ward, J.W.; J. Catal. 11, 238, 1996

Weitkamp, J.; Puppe, L.; (Eds); Catalysis and Zeolites, Fundementals and Applications Springer-Verlag Berlin Heidelberg 1999, preface

Weitkamp, J.; "Zeolites and Catalysis" Solid state Ionics 131 (2000) 175-188

Yang, S.-M.; Lin, J.-Y.; Guo, D.-H.; Liaw, S.-G.; "1-Butene isomerization over aluminophosphate molecular sieves and zeolites" Applied Catalysis A: General 1999, 181:1:113-122